STRIATAL FUNCTION IN FRAGILE X SYNDROME

A Thesis

by

MEGAN CHRISTIANNA DAVIS

Submitted to the Office of Graduate and Professional Studies of
Texas A&M University
in partial fulfillment of the requirements for the degree of

MASTER OF SCIENCE

Chair of Committee,	Laura N. Smith
Committee Members,	William Griffith
	Scott V. Dindot
Head of Department,	Carol Vargas

May 2020

Major Subject: Medical Sciences

ABSTRACT

Fragile X syndrome (FXS) is the leading genetic cause of autism caused by a mutation of the *Fmr1* gene. This mutation results in the loss of fragile X mental retardation protein (FMRP) which associates with and regulates four percent of brain mRNAs. Symptoms associated with FXS in humans range from physical characteristics, such as enlarged ears and pronounced forehead and chin, to behavioral characteristics, such as stereotypies and social deficits. Using total fragile X mental retardation 1 knockout (*Fmr1* KO) mice, a model for FXS, and/or conditional *Fmr1* KO mice, social and natural reward behavioral assays were performed, followed by RNA and protein analyses of FMRP targets with known roles in synaptic function, to further define these characteristics. Results from these experiments showed a trend towards significant social deficits in mice lacking FMRP specifically in cholinergic neurons. Protein analysis revealed differences of expression across cytosolic and synaptic fractions for activity-regulated cytoskeleton-associated protein (ARC), Ras-related C3 botulinum toxin substrate 1 (RAC1), postsynaptic density-95 (PSD-95), as well as for an unidentified band labeled by the ARC antibody. Quantitative (q)PCR analysis identified differences of expression at the RNA level for targets diacylglycerol kinase kappa (*Dgkκ)* and SH3 and multiple ankyrin repeat domains 2, or *Shank2*. Overall, these results point to a possible role for FMRP in cholinergic cells in elements of social behavior and raise questions about its role at translational and transcriptional levels.

DEDICATION

To all my family and friends who have supported me along the way. Without whom none of this would have been possible. In that manner, this is as much a culmination of y'all's hard-work and perseverance as well as mine. Thank y'all.

ACKNOWLEDGEMENTS

I would like to thank my committee chair and mentor, Dr. Smith, for her patience, guidance and support, without whom, I wouldn't be where I am today. I am ever so grateful I was allowed to be a member of her lab, in which I was able to discover the ever fascinating, confusing, and wonderfully frustrating world of fragile X syndrome. I would also like to thank my committee members, Dr. Griffith and Dr. Dindot, for the patience, advice and support throughout this process.

I would also like to thank the members of the Smith lab. Jessica, you have been a great colleague and an even better friend. Without you, this wild ride called grad school would not have been the same. Gia, it's been a wonderful experience being your mentor. I hope you have learned as much from me as I have from you. Catherine, you were always willing to lend a hand around the lab, even if it didn't pertain to your project, thank you for that. Kitzia and Elsbeth, in the limited time that we worked together, I learned you are both quick learners and hard-workers, two traits that I relied upon to assist me through a hectic week, thank y'all for that. I would also like to thank the remainder of the Smith lab: Corinne, David, Carolina, Dottie and Alp.

I would also like to extend my gratitude to my friends and colleagues and to the department faculty and staff for making my time at Texas A&M University a great experience. I would like to specifically thank Nihal, Marissa and Sara. Nihal, I cannot

thank you enough for your patience with my never-ending questions. Marissa, thanks for being a sounding board for me to bounce ideas off of, as well as for helping me learn to use new machines. Sara, thanks for being a great friend. I cannot thank you enough for your support and help throughout this experience.

I would also like to thank a group of people, without whom my life would not have been the same. These individuals are former colleagues, supervisors and mentors. Most importantly, however, they are people I am honored to call friends. Thank you, Dr. Olafson, for giving me an opportunity that changed my life and continuing your support and assistance whenever I ask. Thank you, Dr. Temeyer, for continuing that opportunity and providing support. Thank you, Kylie, for your support not only throughout my professional, but personal, life as well. Also, Greta, I cannot thank you enough for your mentorship in the lab when I first started. Kristie, thank you so much for your friendship and support throughout this journey. Anytime I had any questions, concerns or just needed to talk, I knew I could count on you. To this amazing group of individuals, thank you does not even begin to cover the gratitude I have for each of y'all. Each of you have helped shape me into the researcher I am today and without you, I would not have even made it this close to reaching my goals.

Lastly, but certainly not least, I would like to thank my family. Starting with my grandparents, I will be eternally grateful for all the support y'all have provided throughout not just this experience but throughout my life. You not only made sure that I

had dreams and goals, but you made it possible for me to pursue them. I would like to thank my mother. You have taught me many valuable lessons about life and the person I want to be. I am who I am today and where I am because of what you've taught me. I hope I can be half the person you are. I would also like to extend my gratitude to my aunts and uncles and cousins, who due to their support and assistance has allowed me to chase my dreams. To this group of people that I call family, thank you seems so inadequate, so I'll just say love y'all instead.

CONTRIBUTORS AND FUNDING SOURCES

Contributors

This work was supervised by a thesis committee consisting of Dr. Laura Smith, Chair, and Dr. William Griffith of the Department of Neuroscience and Experimental Therapeutics, as well as Dr. Scott Dindot of the Department of Veterinary Pathobiology and Department of Cellular and Molecular Medicine.

Data analysis for social CPP, as well as for western blotting, was conducted in part by Dr. Laura Smith. Gia Valles assisted with tissue preparation, SDS-PAGE and western blotting. Kitzia Corona and Elsbeth Chow assisted with qPCR. All other experiments were performed and data analyzed independently by the student.

Funding Sources

These studies were made possible by internal funding from Texas A&M University, including a T3, Triads for Transformation Award (Project ID 1010).

NOMENCLATURE

Arc	Activity-regulated cytoskeleton-associated protein
ASD	Autism Spectrum Disorder
CPP	Conditioned Place Preference
Dgkκ	Diacylglycerol kinase kappa
DST	Dorsal Striatum
FMRP	Fragile X Mental Retardation Protein
FXS	Fragile X Syndrome
KO	Knockout
NAc	Nucleus Accumbens
PSD-95	Postsynaptic density-95
RAC1	Ras-related C3 botulinum toxin substrate 1
sCPP	Social Conditioned Place Preference
Shank2	SH3 and multiple ankyrin repeat domains 2
WT	Wild Type

TABLE OF CONTENTS

Page

LIST OF FIGURES

Page

1. INTRODUCTION

Fragile X syndrome (FXS) is the leading monogenic cause of autism spectrum disorder (ASD), occurring in roughly one in 4,000 males and one in 8,000 females (Kolehmainen, 1994; Turner, Webb, Wake, & Robinson, 1996; Westmark & Malter, 2007; Winter, 1987) (reviewed in (Garber, Smith, Reines, & Warren, 2006). It is estimated that approximately 50 percent of the FXS population also falls into the ASD population and accounts for five percent of all ASD diagnoses (Demark, Feldman, & Holden, 2003; Kaufmann et al., 2004; Kaufmann et al., 2017). FXS is the result of a mutation in the 5' untranslated region caused by the extension of a CGG trinucleotide region, located on the X chromosome on locus Xq27.3 (Krawczun, Jenkins, & Brown, 1985; Pieretti et al., 1991). In the general population, the CGG repeat occurs between six and 54 times, whereas in the affected population over 200 repeats are present (Fu et al., 1991). The expansion of this trinucleotide repeat results in the promoter region of the fragile X mental retardation 1 (*Fmr1*) gene becoming hypermethylated, thereby silencing its expression (Pieretti et al., 1991).

Fmr1 encodes the fragile X mental retardation protein (FMRP), which acts as a RNA binding protein and associates with approximately four percent of total brain mRNAs (Ashley, Wilkinson, Reines, & Warren, 1993; Brown et al., 2001). FMRP contains three RNA binding domains—an RGG box plus two K homology domains, KH1 and KH2 (Siomi, Siomi, Nussbaum, & Dreyfuss, 1993)—as well as nuclear export and nuclear

localization signals (Bardoni, Sittler, Shen, & Mandel, 1997; Eberhart, Malter, Feng, & Warren, 1996) . Along with other RNA-binding proteins, FMRP binds with mRNA and forms a ribonucleoprotein complex, which is transported to the cytoplasm and associates with polyribosomes (Corbin et al., 1997; Eberhart et al., 1996). In its phosphorylated state, FMRP inhibits translation of its mRNA targets (Ceman et al., 2003; Narayanan et al., 2007; Zalfa et al., 2003), so that, at least in some brain regions, loss of FMRP is associated with increased basal protein synthesis (Osterweil, Krueger, Reinhold, & Bear, 2010; Qin, Kang, Burlin, Jiang, & Smith, 2005). Activation of mGluR5 receptor signaling leads to dephosphorylation of FMRP (Ceman et al., 2003; Narayanan et al., 2007) and release of translational repression (Chuang et al., 2005; Huber, Gallagher, Warren, & Bear, 2002). The mechanism by which FMRP mediates translation has been debated (Chen, Yun, Seto, Liu, & Toth, 2003; Laggerbauer, Ostareck, Keidel, Ostareck-Lederer, & Fischer, 2001; Li et al., 2001; Miyashiro et al., 2003; Todd, Mack, & Malter, 2003). FMRP has also been shown to suppress translation by interaction with the RNA-induced silencing complex (RISC) (Ravi et al., 2011).

Many of FMRP's targets are involved in synapse regulation, including their structure and function (Darnell et al., 2011; Edbauer et al., 2010; Pfeiffer et al., 2010), and thus, there are numerous reported effects on dendritic spines, the postsynaptic structure for excitatory synapses, in both humans and mice lacking FMRP (Comery et al., 1997; Dictenberg, Swanger, Antar, Singer, & Bassell, 2008; Dölen et al., 2007; Irwin et al., 2001; Rudelli et al., 1985; Smith et al., 2014; Tabet et al., 2016). A few of these targets

are the activity-regulated cytoskeleton-associated protein (Arc) (Niere, Wilkerson, & Huber, 2012), diacylglycerol kinase kappa (DGKK) (Tabet et al., 2016), SH3 and multiple ankyrin repeat domains 2 (SHANK2) (Korb et al., 2017), as well as Ras-related C3 botulinum toxin substrate 1 (Rac1) (Castets et al., 2005), all of which play regulatory roles in synapse formation, maturation, and/or maintenance, or otherwise control aspects of synapse strength or dendritic morphology (Peebles et al., 2010; Tabet et al., 2016; Tashiro & Yuste, 2004; Zaslavsky et al., 2019).

Loss of FMRP results in multiple physical, cognitive and neurophysiological characteristics. Common physical features include prominent jaw, protruding forehead, enlarged ears, long narrow face, and in males, macro-orchidism (Randi Jenssen Hagerman & Hagerman, 2002; R. J. Hagerman, Van Housen, Smith, & McGavran, 1984). Behavioral and cognitive impairments, common in the fragile X population, include intellectual disabilities(Ballinger, Cordeiro, Chavez, Hagerman, & Hessl, 2014; de Vries et al., 1996), obsessive compulsive disorder (Berry-Kravis & Potanos, 2004), anxiety (Bregman, Leckman, & Ort, 1988; Cordeiro, Ballinger, Hagerman, & Hessl, 2011), aggression (Berry-Kravis & Potanos, 2004; Cohen, 1995), attention deficit/hyperactivity (R. Hagerman, Kemper, & Hudson, 1985), restricted interests and motor stereotypies (Borghgraef, Fryns, Dlelkens, Pyck, & Berghe, 1987; Cohen et al., 1988), and social deficits (Cohen et al., 1988; Cordeiro et al., 2011). Restricted behaviors, stereotypies, and impaired social functioning, in particular, have been tied functionally to the striatum, a brain region involved in learning, memory, motor

function, and reward behavior (Balleine, Liljeholm, & Ostlund, 2009). The striatum is divided into dorsal and ventral regions, and both consist of multiple cell types (Y. Kawaguchi, 1997; Yasuo Kawaguchi, Wilson, Augood, & Emson, 1995). Medium spiny neurons (MSNs) make up 90 to 95 percent of striatal cells (Briones, Tang, Haye, & Gould, 2018; Yasuo Kawaguchi et al., 1995). Fast-spiking GABAergic interneurons, which make up about three percent of the striatal cells (Tepper, Tecuapetla, Koós, & Ibáñez-Sandoval, 2010), can be divided into three subcategories, parvalbumin-containing, somatostatin-containing, and calretinin-containing (Y. Kawaguchi, 1997). Cholinergic interneurons are the remaining interneuron category and represent around two percent of the striatal cell population (Zhou, Wilson, & Dani, 2002). These interneurons are the primary source of acetylcholine (Ding, Guzman, Peterson, Goldberg, & Surmeier, 2010; Goldberg, Ding, & Surmeier, 2012; Wang et al., 2006). Interestingly, disruption of the cholinergic system can lead to behaviors similar to those associated with FXS (Abitbol et al., 1993; Chang et al., 2008; D'Antuono, Merlo, & Avoli, 2003; Greicius, Boyett-Anderson, Menon, & Reiss, 2004; Sarter, Bruno, & Givens, 2003). For instance, deletion of both fast-spiking GABAergic and cholinergic interneurons in the striatum increased stereotypy, anxiety and social deficits in otherwise normal male, but not female, mice (Rapanelli et al., 2017). In the BTBR T+tf/J mouse model for ASD, which has lower levels of acetylcholine, inhibiting acetylcholinesterase improved social deficits and cognitive rigidity (Karvat & Kimchi, 2014).

In this project, my goal is to better understand how loss of FMRP contributes to ASD-related behavior, namely deficits in social preference. For this purpose, I have conducted social conditioning behavioral assays in a mouse model for FXS and in mice lacking FMRP in cholinergic cells brain-wide, comparing each to control littermate mice. Following social conditioning and testing, I examined targets of FMRP identified from previous research at both RNA and protein levels in each group. By isolating particular targets, including *Dgkκ* and *Arc*, as well as identifying reward-related behavior associated with each group, the role of striatal FMRP in the regulation of translation during social experience is further elucidated.

2. METHODS

2.1. Animals and Handling

Fmr1$^{-/y}$ and *Fmr1*$^{-/+}$ mice (Jackson Laboratory, Stock # 003025) maintained on a C57BL/6N (Charles River) background for more than 25 generations were bred to produce wildtype (WT) and *Fmr1* knockout (KO) male littermate mice. In addition, ChAT-Cre BAC transgenic mice were bred with floxed-*Fmr1* mice to produce male ChAT$^{+/Tg}$; *Fmr1*$^{fl/y}$ mice, which were bred to female ChAT$^{+/+}$; *Fmr1*$^{fl/fl}$ mice to produce ChAT$^{+/Tg}$ and ChAT $^{+/+}$ fully floxed-*Fmr1* male and female offspring. Prior to the start of each behavioral assay, mice were handled over the course of three days, increasing from free handling to brief restraint, and were acclimated in the experimental room in home cages ($\geq$1 hr) each day prior to testing.

2.2. Social Conditioned Place Preference

Each conditioned place preference (CPP) box (Appendix Figure A.1) consisted of three chambers, with two main chambers having either white and black alternating striped walls and small wire-grid flooring or grey walls and larger wire-grid flooring. A neutral chamber having all white walls and metal bar flooring allowed travel between the main chambers during pre- and post-test sessions (20 min) via open doors. Doors were unavailable during the conditioning phase when mice were alternately sequestered in each main chamber over eight sessions (20 min; 1/day), one having the social stranger under an inverted wire cup and one having only an empty inverted wire cup. Time spent in each and distance traveled throughout the chambers were tracked using infrared

cameras and Ethovision (Noldus) software over the entire experiment. Manual scoring of the video was used to check and correct the automated tracking. On pre- and post-test days, the test animal was placed in the middle of the neutral chamber to start the trial. Each animal's pre-test score was calculated by subtracting time spent in one main chamber from the other. Choice of the grey or striped chamber to be paired with the social condition followed a balanced design, such that 1) group averages of pre-test preferences for the social-paired chamber were as close to each other and 2) to zero as possible, while 3) using both chambers equivalently. Before and after each trial, chambers were cleaned with 70% ethanol.

2.3. Food Operant Behavior

Testing, which consisted of acquisition, extinction, re-acquisition, and dose response phases, took place in operant conditioning chambers (Appendix Figure A.2) for 2 hr sessions daily (5 days/wk). Each chamber contained two nose poke ports located on either side of a magazine containing a liquid dipper (Appendix Figure A.3), which was made accessible for 60 sec following reinforced nose pokes into the active port. Visits to ports and the magazine were monitored by infrared beam. After each 2-hr trial, animals were immediately removed from each chamber and placed back into their home cage. Between trials, waste trays and liquid food troughs were washed in scentless soapy water. During the acquisition phase of the task, nose pokes into the predetermined active port resulted in a liquid food reward (25 ul, 100% Ensure®, vanilla-flavored) offered in the central magazine. Acquisition criteria were met when the animal made $\geq$20 reinforced (active) nose pokes with $\geq$70 percent preference ((active/ (active + inactive

port pokes)) *100) for the active port over two consecutive days. During extinction, trials were the same except the liquid reinforcer was replaced with water. Extinction criteria were met when, compared to the average of their last two days of acquisition, an animal's reinforced nose pokes were reduced by half for two consecutive days.

Following extinction, Ensure® (100%) was again used as the reinforcer for re-acquisition of the task, and when the animal made $\geq$20 reinforced active responses within a session (typically achieved within two sessions), dose response testing began the following test day. Dose response consisted of two consecutive days at each of several concentrations of Ensure® (zero, three, 10, 32, and 100%; diluted in water) as the reinforcer. Latin Square design was used to determine the starting reinforcer concentration for each animal, which was followed by the next incremental dose until all doses were completed.

2.4. Tissue Dissection

To quantify proteins within brain regions, animals were killed by live decapitation, and using chilled instruments, the brain removed from the skull, and sliced (1 mm coronal sections). The dorsal striatum, between Bregma 1.54 mm and 0.14 mm, and the nucleus accumbens, between Bregma 1.54 mm and 0.62 mm, were hand-dissected from two slices, each.

2.5. Synaptosome Preparation and Western Blotting

Synaptosomes were prepared from each brain region from individual mice. Briefly, using a handheld pellet pestle mixer, samples were lysed in Syn-PER Synaptic Protein

Extraction Reagent (ThermoFisher 87793) containing 1X cOmplete EDTA-free Protease Inhibitor Cocktail (Roche). After centrifugation (1200 x g for 10 min), a small amount of the supernatant (homogenate; S1) was reserved. The remainder was centrifuged (15,000 x g for 20 min) to produce the second supernatant (cytosolic fraction; S2) and a pellet, which was resuspended in Syn-PER according to manufacturer directions as the synaptosome fraction (P2). A minimal amount of each fraction was then used for protein quantification (DC Protein Assay Kit, BioRad) and equal amounts of total protein (40 ug/well) or (10 ug/well) were run on homemade sodium dodecyl sulfate-polyacrylamide (SDS-PAGE) acrylamide gels (8%) at 100 V for approximately 1.5 hrs or until the bottom of the ladder reached the bottom of the gel. Separated proteins were transferred to a polyvinylidene fluoride (PVDF) membrane (iBlot Gel Transfer stacks, Invitrogen IB401001) using the Invitrogen iBlot transfer system, set to the manufacturer's preprogramed protocol number 3 (20 V for 7 min). Blots were blocked in casein blocking buffer (LI-COR 927-40200) for 1 hr, then placed in primary antibody diluted in casein buffer overnight at 4°C with gentle shaking. Incubation in secondary antibody (diluted in casein buffer with 0.01% SDS and 0.2% Tween) was performed at room temperature for 1 hr before rinsing in TBS-T and imaging (LI-COR). Primary antibodies were anti-ARC (Synaptic Systems 156-002, 1:2000), anti-RAC1 (EMD Millipore 05-389, 1:1000), anti-PSD-95 (Millipore Sigma MABN68, 1:1000), anti-DGKK (Abcam ab94575, 1:1000), anti-DGKK (ABgent AP122b, 1:500), anti-GAPDH (Fisher-Scientific AM4300, 1:1000), and anti-FMRP (Abcam ab17722, 1:1000). Secondary antibodies were IRDye 680RD goat anti-mouse IgG polyclonal (LI-COR 926-68070, 1:20000),

IRDye 800RD goat anti-mouse IgG polyclonal (LI-COR 926-32210, 1:20000), or IRDye 800RD goat anti-rabbit IgG polyclonal (LI-COR 926-32211, 1:20000). All primary targets of interest were normalized to GAPDH expression in the same lane prior to further analyses.

2.6. Primer Design

To design primers for genes of interest, transcripts were used to identify each exon and intron using the NCBI database. Primers were then designed to span exon-to-exon junctions, with reverse primers targeted to an exon subsequent to the forward primer. More specifically, the sequences of all exons were separated from the intron sequences using the FASTA transcript and the genomic regions marked on the NCBI gene page. Transcripts of single exons were plugged into the Primer3 website to generate potential forward and reverse primers. The potential primer sequences were then plugged into the free Beacon Designer website to determine dimer potentials. Primers with greater than four, for any of the dimer possibilities were eliminated. Primer sequences were also assessed using Primer Blast using the same standards. Primers are listed in Supplemental D.

2.7. RNA Analysis

Isolated brain regions from individual mice were either flash frozen in liquid nitrogen and stored at -80°C for later processing or used immediately for RNA isolation (Zymo Research Microprep kit, R1050), cDNA synthesis (Quantabio qScript cDNA synthesis kit, 95047-100), PCR using Pfu Turbo DNA polymerase (Agilent, 600250) and qPCR using SYBR Green (Applied Biosystems, 43-444-63). Temperature (50, 53, 55, and 60°

C), and concentration (50 ng, 25 ng, and 10 ng per reaction) gradients were conducted for each primer set by basic PCR using Pfu Turbo to amplify genes of interest, and products were electrophoresed on an agarose gel (2%) to confirm proper band size. After optimization, synthesized cDNA was then used to run qPCR (Applied Biosystems Vii A7). All samples were run in triplicate. Using the cycle threshold (ct) method, mean ct was used to calculate the fold change of each protein after normalizing to GAPDH. If any sample had a ct standard deviation greater than 0.5, the sample that varied the most was removed and a new ct average was calculated. After quantification, PCR products were run on an agarose gel (2%) to confirm band size.

2.8. Immunohistochemistry (IHC)

Whole brains were removed from the skull, lightly fixed in paraformaldehyde (PFA; 4%; 24 hrs), and cryoprotected in sucrose solution (30%; 48 hours or until the brain sank) before slicing on a microtome (40 um). Slices were serially incubated in anti-FMRP (abcam ab17722, 1:500) followed by AlexaFluor568 donkey anti-rabbit (abcam ab175470, 1:200), then goat anti-choline acetyltransferase (ChAT) polyclonal antibody (Millipore AB144P, 1:100) primary followed by AlexaFluor647 donkey anti-goat (Fitzgerald 43R-ID028AF, 1:200). Slices were mounted onto a microscope slide and imaged (40X) using a motorized inverted microscope (Olympus IX83) with confocal scanning head (Fluoview FV1200).

2.9. Statistics

Statistical analysis was performed in GraphPad Prism or SPSS. In operant conditioning, animals took different numbers of days to meet the criteria during each phase, thus the

first and last days were analyzed alone, with port (active, inactive) as a repeated measure, using Two-Way Mixed ANOVAs. CPP scores from the pre- and post-tests were analyzed as repeated measures using Two-Way Mixed ANOVAs (test x genotype). For western blotting of cellular fractions, fluorescent signals on LI-COR images were quantified (ImageStudio Lite, version 5.2). Expression of each protein in the S1 fraction (total homogenate) was verified not to differ between genotypes using independent samples t-tests. S2 and P2 fractions were then normalized to the corresponding WT S1 fraction and analyzed using separate Two-Way Mixed ANOVAs (genotype x fraction) for each protein. For qPCR, independent samples t-tests were ran to compare the fold change of each gene target between genotypes. All graphs display the mean ± S.E.M.

3. RESULTS

3.1. *Fmr1* Total KO (FXS) Mouse Line

3.1.1. Behavioral Testing

3.1.1.1. Social conditioned place preference

After conditioning, *Fmr1* KO mice (n=24) reduced, while WT mice (n=26) increased, the amount of time spent in the social-paired chamber, in general. However, the two groups did not differ significantly from one another in their CPP scores at the post-test, nor did either group differ significantly in time spent in the social-conditioned chamber at post-test compared to their own pre-test (Figure 1). When looking at the entries into the social-paired chamber, there is a significant difference between the pre- and post-tests, due to an increase in entries during the post-test across both genotypes (Two-Way Mixed ANOVA, main effect of test session, $F_{1,48} = 24.61$, $p<0.0001$), an effect that remained significant for both *Fmr1* KO and WT groups (Figure 2; Bonferroni post-hoc comparisons: WT, $p<0.0001$; KO, $p<0.05$). In addition, there was a significant difference between pre- and post-test entries into the unpaired (non-social) chamber (Two-Way Mixed ANOVA, $F_{1,48} = 26.50$, $p<0.05$), again due to an increase in post-test entries, an effect that persisted when looking at each genotype individually (Figure 3; Bonferroni post-hoc comparisons: WT, $p<0.001$; KO, $p<0.01$).

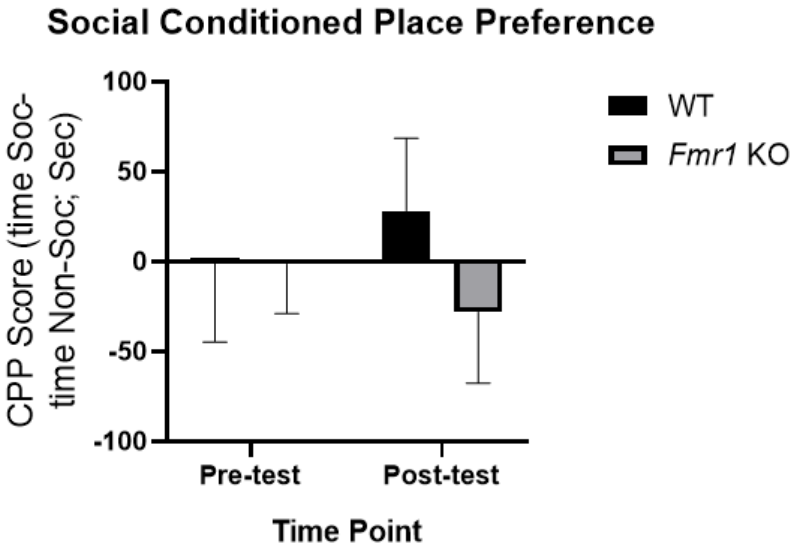

Figure 1: *Fmr1* WT vs KO mice comparing the pre- and post-test scores. Two-way Repeated measures (RM) ANOVA. KO: n=24; WT: n=26. Data shown are mean ± SEM.

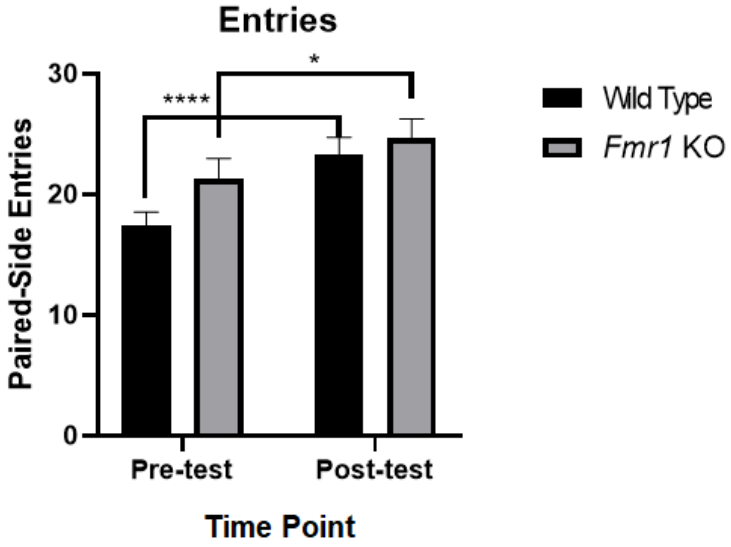

Figure 2: Paired chamber entries comparing pre- and post-test of *Fmr1* WT and KO mice. Two-Way Mixed ANOVA. *p<0.05, ****<0.0001. KO: n=24; WT: n=26. Data shown are mean ± SEM.

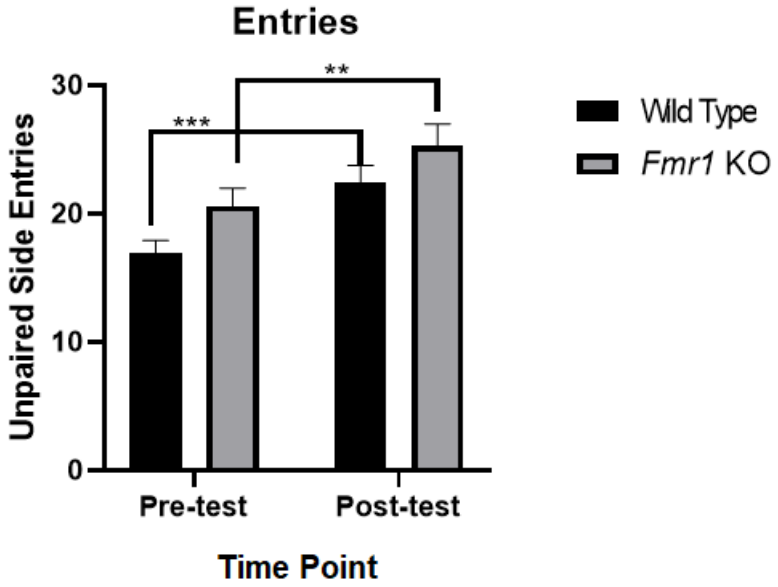

Figure 3: Comparison of number of entries between pre- and post-tests of *Fmr1* WT and KO mice, into the unpaired conditioning chamber. Two-Way Mixed ANOVA. **p<0.01, ***<0.001. KO: n=24; WT: n=26. Data shown are mean ± SEM.

3.1.1.2. Food operant behavior

As described, animals were moved through acquisition and extinction phases based on performance (meeting phase criteria) rather than the number of days, meaning that individual mice differed in the number of days spent in these phases. Importantly, all animals (9 WT, 11 KO) met acquisition phase criteria within 12 days, and there was no significant difference in the number of days required to reach criteria by WT and *Fmr1* KO mice (Figure 4, inset). In addition, there was no significant difference in the number of active nose pokes made on either the first day or over the last four days between KO and WT mice (Figure 4; independent samples t-test, 2-tailed, $t_{18} = 0.4291$, $p=0.673$; Two-Way Repeated Measures (RM) ANOVA, $F_{3,54}=10.55$, $p<0.0001$, respectively).

Following acquisition was extinction. All animals met extinction criteria within eight days, and there was no significant difference in the amount of days it took the groups to reach extinction criteria (Figure 5, inset). Although, there was no significant difference in the number of active port nose pokes between groups on the first day of extinction, there was a trend towards a significant difference in this measure on the last day of extinction (Figure 5; independent samples t-test, 2-tailed, $t_{18} = 2.053$, $p=0.0549$), where *Fmr1* KO mice made more active port nose pokes than their WT counterparts. For re-acquisition, when reinforcer was again made available during the task for active nose pokes, there was no significant difference in the amount of days it took for the genotypes to reach criteria; all animals met criteria for re-acquisition within four days. Groups also did not differ significantly on the number of reinforcers earned on the first or last day of re-acquisition (Figure 6). During dose response testing, genotypes did not differ significantly in their active port responses over five reinforcer concentrations (Figure 7).

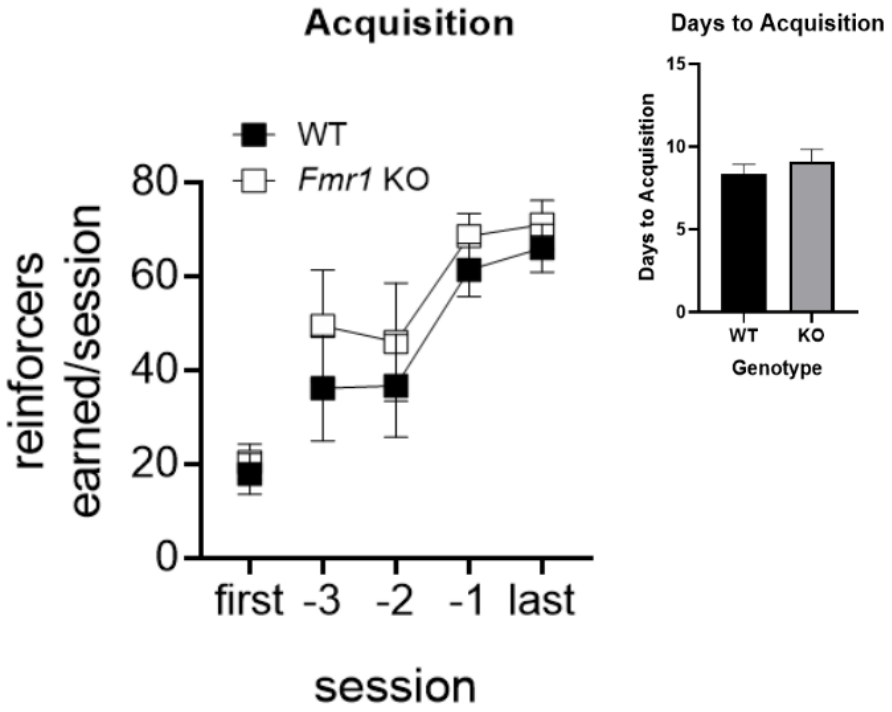

Figure 4: Acquisition of *Fmr1* KO vs. WT animals during 1st and last 4 days, as well as the average number of days for groups to reach criteria. Independent samples t-test (2-tailed) on 1st days, Two-way RM ANOVA on last 4 days. Data shown are mean ± SEM. KO: n=9; WT: n=11.

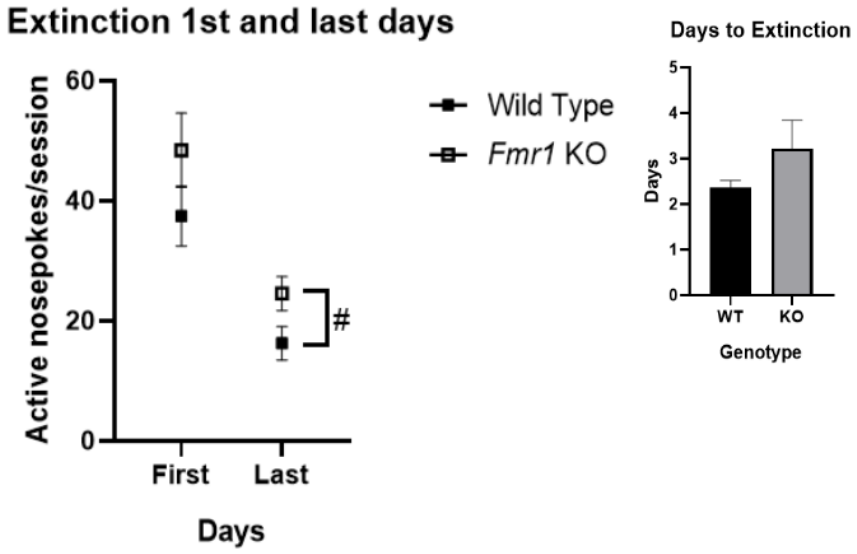

Figure 5: Average number of active nose pokes by genotype on 1st and last days of extinction. Also, the average number of days for each group to reach criteria. Independent samples t-test (2-tailed). #p=0.0549. KO: n=9; WT: n=11. Data shown are mean ± SEM.

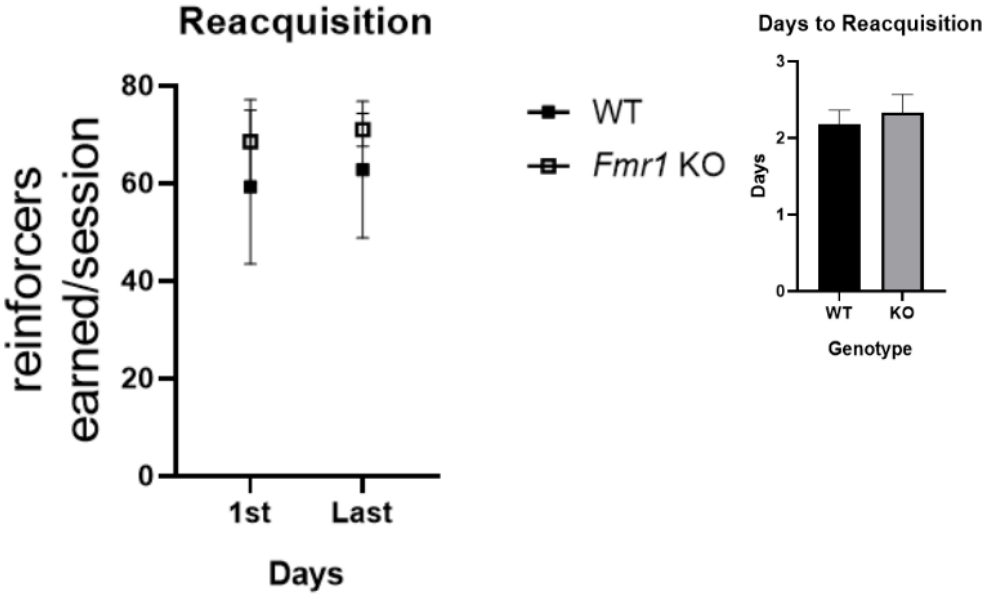

Figure 6**:** Average number of reinforcers earned for each genotype on 1st and last days of reacquisition, along with the average number of days to reach criteria. Independent samples t-tests (2-tailed). KO: n=9; WT: n=11. Data shown are mean ± SEM.

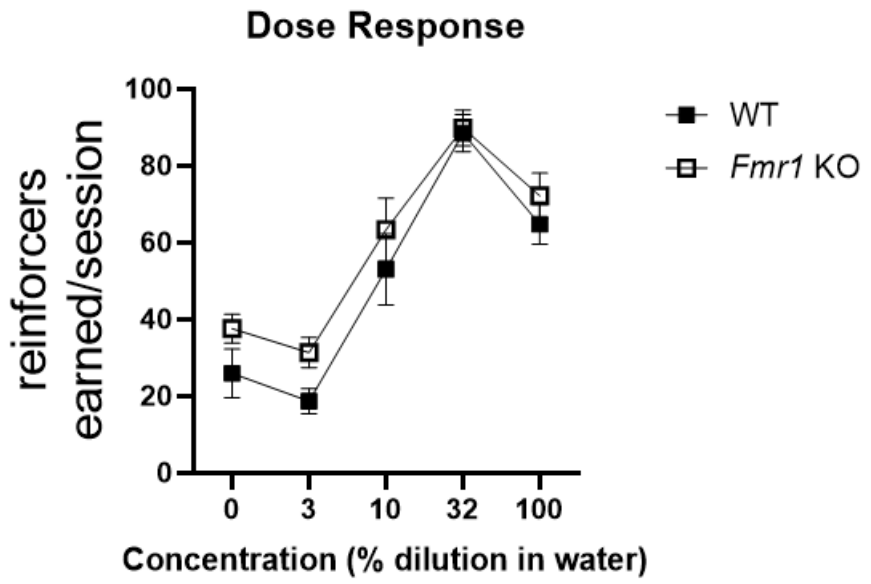

Figure 7: Dose response (Ensure®, vanilla-flavored) for each genotype at each dilution. Two-way RM ANOVA. KO: n=9; WT: n=11. Data shown are mean ± SEM.

3.1.2. Tissue Analysis

3.1.2.1. Social Conditioned Place Preference

Dorsal striatum, as well as the nucleus accumbens, tissue from *Fmr1* KO and WT mice that underwent social CPP were prepared for qPCR. Previously identified targets of FMRP were assessed, including *Arc* (variant 2), *Shank2, Rac1*, and *Dgkκ*. For dorsal striatum, there was a trend towards a significant main effect of genotype for *Dgkκ* expression, with increased expression in the KO animals (Figure 8; Mann Whitney U test, U=4; median WT=11.27, n=4; median KO=10.88, n=4; p=0.0952). Expression of *Rac1*, *Shank2,* and *Arc* did not significantly differ between genotypes.

In the nucleus accumbens, *Arc* and *Rac1* expression between genotypes did not reach the threshold for significance. *Shank2*, however, was significantly increased in the WT group (Figure 9; independent samples t-test, 2-tailed, $t_2 = 10.83$, $p<0.\ 0.01$); however, this analysis had a very small sample size.

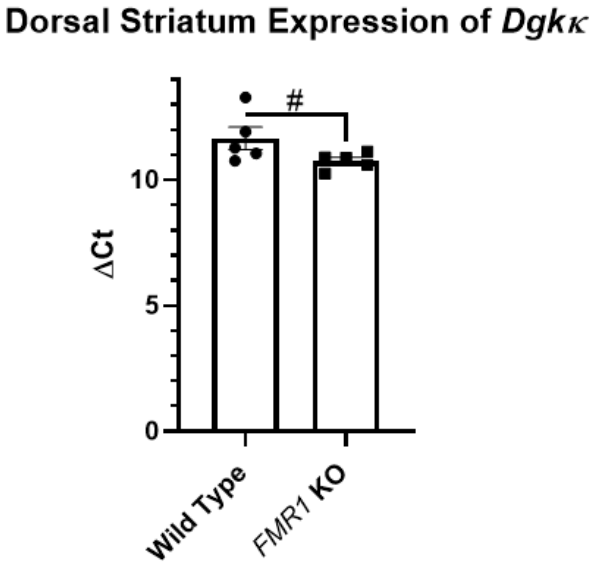

Figure 8: Expression of Dgkκ in the dorsal striatum. Ct values normalized to GAPDH. WT: n=5; KO: n=5. Mann Whitney U Test. #p=0.0952. Data shown are mean ± SEM.

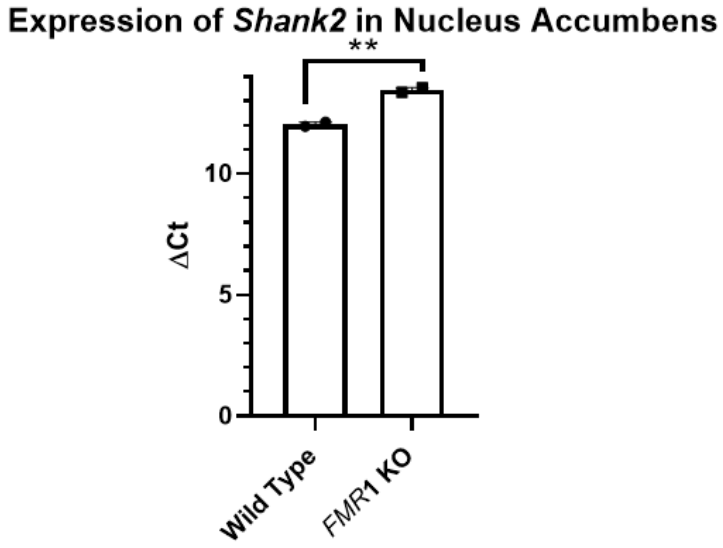

Figure 9: Expression of Shank2 in the nucleus accumbens. Ct values normalized to GAPDH. Unpaired t-test. *p<0.01. WT: n=2; KO: n=2. Data shown are mean ± SEM.

3.1.2.2. Food Operant Conditioning

Tissue from mice that had undergone food operant conditioning was used for synaptosome preparation and western blotting. Protein expression was compared between the S2 (cytosolic) and P2 (synaptosome) fractions, as well as between genotypes, from the dorsal striatum and the nucleus accumbens. Analysis of ARC protein of the 55 kDa size across the S2 and P2 fractions showed main effects of fraction for both dorsal striatum (Figure 10; Two-Way Mixed ANOVA, $F_{1,6} = 9.472$, $p<0.05$) and NAc (Figure 11; $F_{1,6} = 8.452$, $p<0.05$), in both cases due to an increase in P2 ARC expression.

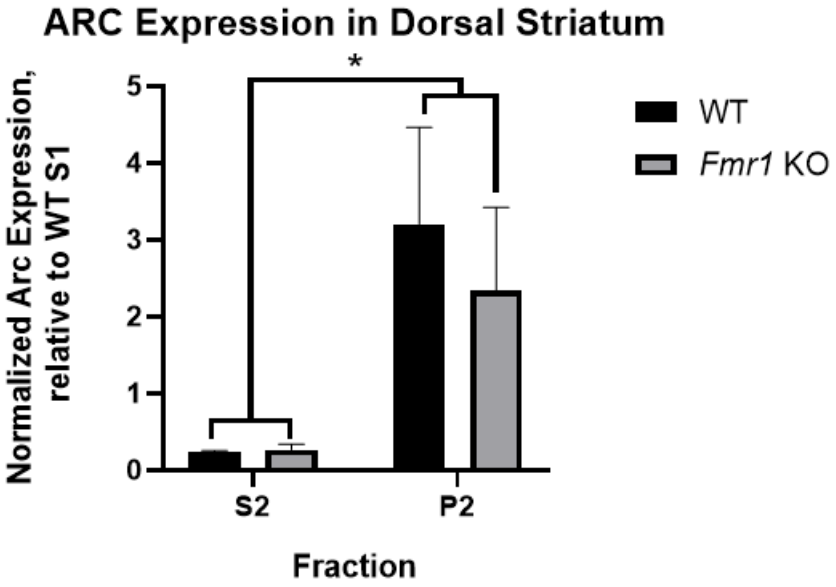

Figure 10: Comparison of ARC expression in WT and KO animals between fractions. KO: n=4; WT: n=4. Two-Way Mixed ANOVA. *p<0.05. Data shown are mean ± SEM.

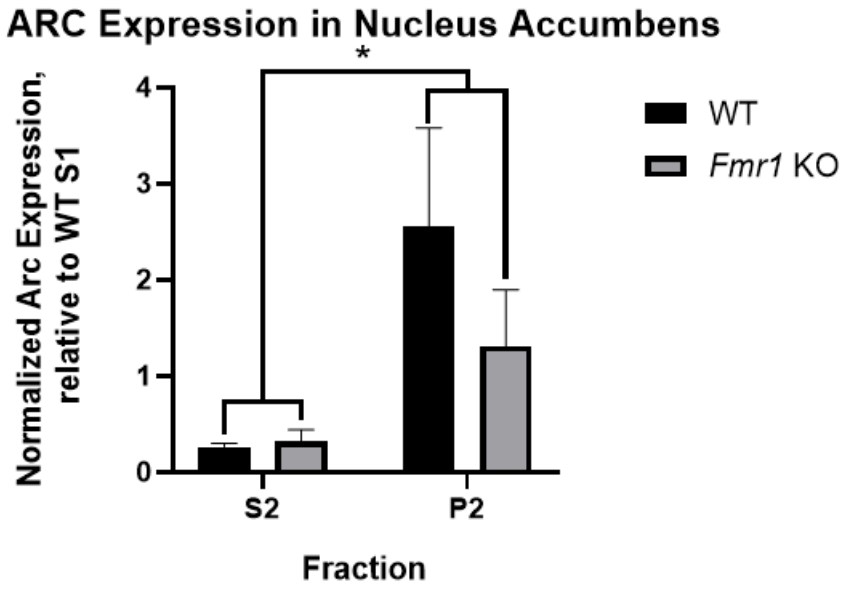

Figure 11: Comparison of ARC, within the NAc region across S2 and P2 fraction. KO: n=4; WT: n=4. Two-Way Mixed ANOVA. *p<0.05. Data shown are mean ± SEM.

For ARC, there was also noticeable binding near 130 kDa, resulting in a band that was quantified. In the dorsal striatum, there was significant main effect of fraction found for this band (Figure 12; Two-Way Mixed ANOVA, $F_{1,6} = 32.296$, $p<0.001$) due to decreased expression in the P2 fraction compared to the S2 fractions, and this effect was significant within each genotype (Bonferroni post-hoc comparisons: WT, $p< 0.01$; KO, $p<0.05$). Analysis of this same band from NAc tissue showed a significant interaction between genotype and fraction (Figure 13; Two-Way Mixed ANOVA, $F_{1,6} = 8.921$, $p<0.05$). Follow-up analyses (Univariate ANOVAs) revealed a significant difference between genotypes for the cytosolic (S2) ($p<0.05$), but not the synaptosomal (P2), fraction, with KO mice having higher expression than WT. There was also a significant simple main effect of fraction in the KO group ($p<0.05$), where S2 expression was greater than P2, while only a trend towards a significant main effect of fraction was observed in the WT group (Figure 14).

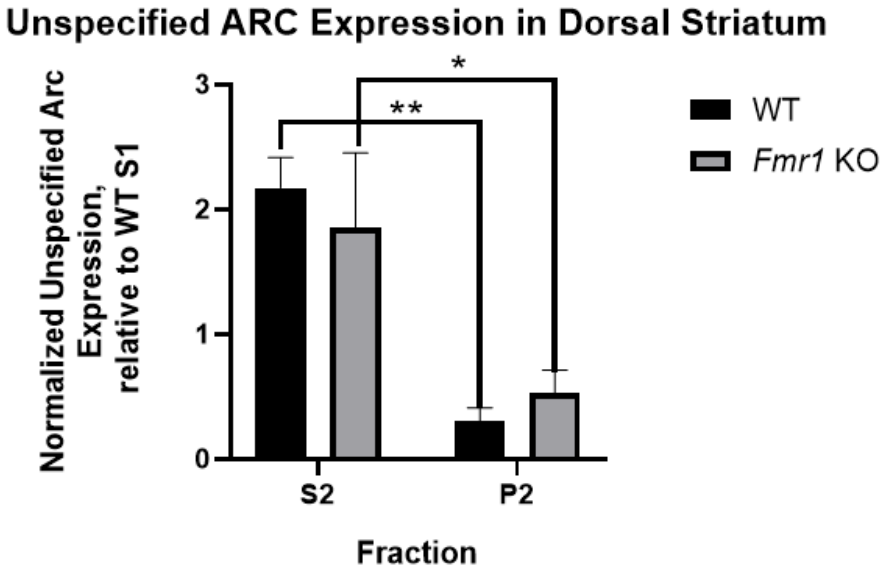

Figure 12: Expression of non-specific ARC band within dorsal striatum region. KO: n=4; WT: n=4. Bonferroni post-hoc comparison. *p<0.05, **p<0.01. Data shown are mean ± SEM.

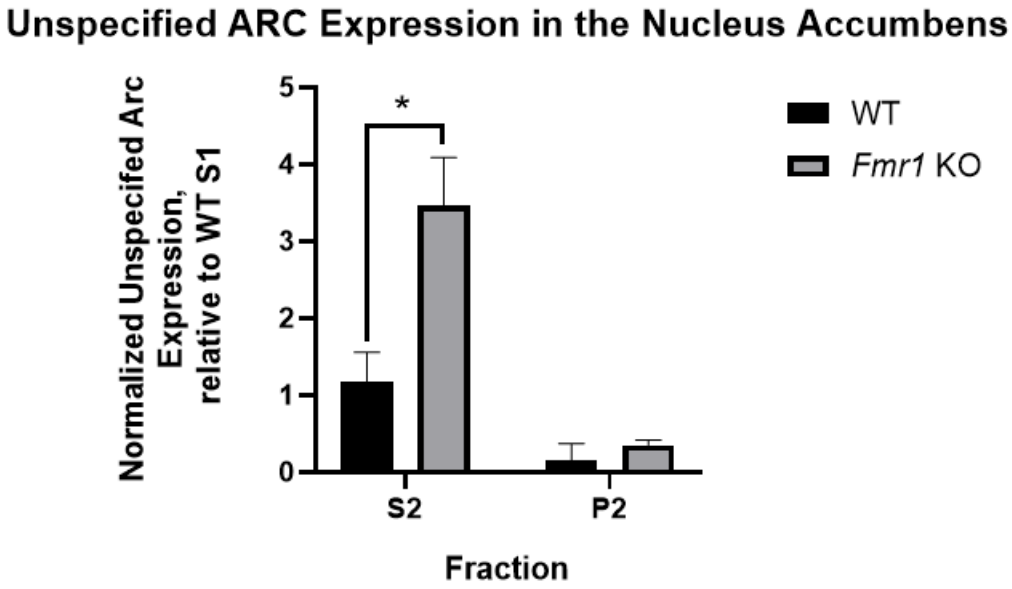

Figure 13: Expression of non-specific ARC band across fractions within genotype. KO: n=4; WT: n=4. Two-Way Mixed ANOVA with Univariate ANOVA follow-up. *p<0.05. Data shown are mean ± SEM.

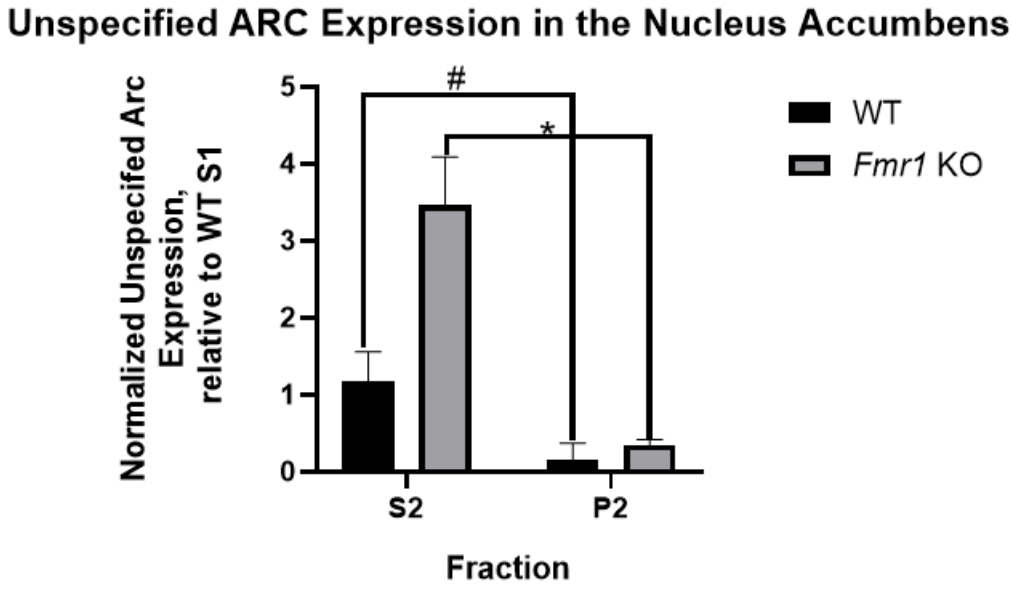

Figure 14: Expression of non-specific ARC band within NAc region across fractions. KO: n=4; WT: n=4. Two-Way Mixed ANOVA. *p<0.05, #=0.092. Data shown are mean ± SEM.

For PSD-95 in the dorsal striatum, there was a trend towards a significant main effect of fraction (Figure 15; Two-Way Mixed ANOVA, $F_{1,5} = 4.305$, p=0.093). For PSD-95 expression within the nucleus accumbens, there was a significant main effect of fraction (Two-Way Mixed ANOVA, $F_{1,6} = 18.073$, p<0.01), and further analysis revealed increased expression within the P2, compared to the S2, fraction for WT and a trend for KO) (Figure 16; Bonferroni post-hoc comparisons: WT, p<0.05; KO, p=0.06). The final protein probed for was RAC1, and there was a significant main effect of fraction in dorsal striatum (Figure 17; Two-Way Mixed ANOVA, $F_{1,6} = 8.247$, p<0.05) and a trend towards a significant main effect of fraction in the nucleus accumbens (Figure 18; Two-Way Mixed ANOVA, $F_{1,6} = 5.509$, p<0.057).

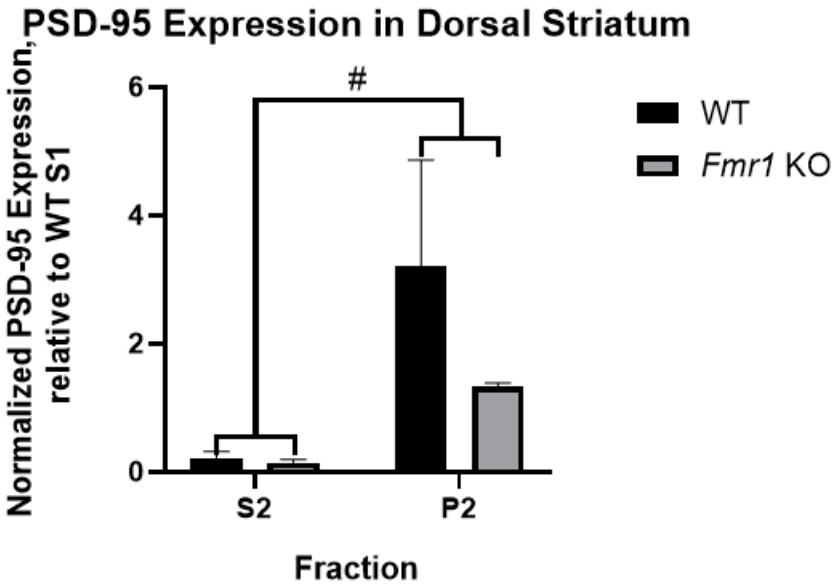

Figure 15: Expression of PSD-95 in the dorsal striatum. KO: n=4; WT: n=4. Two-Way Mixed ANOVA. #=0.052. Data shown are mean ± SEM.

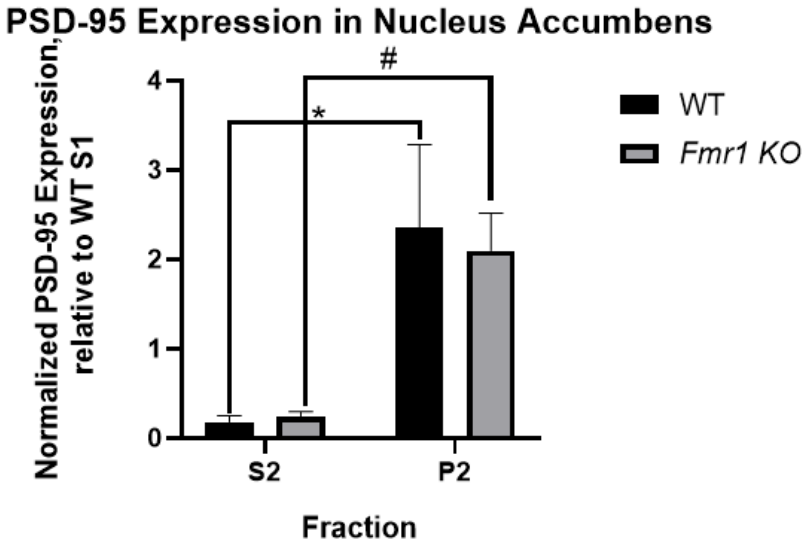

Figure 16: Expression of PSD-95 within the P2 fraction of both genotypes. KO: n=4; WT: n=4. Bonferroni post-hoc comparison. *p<0.05; #p=0.06. Data shown are mean ± SEM.

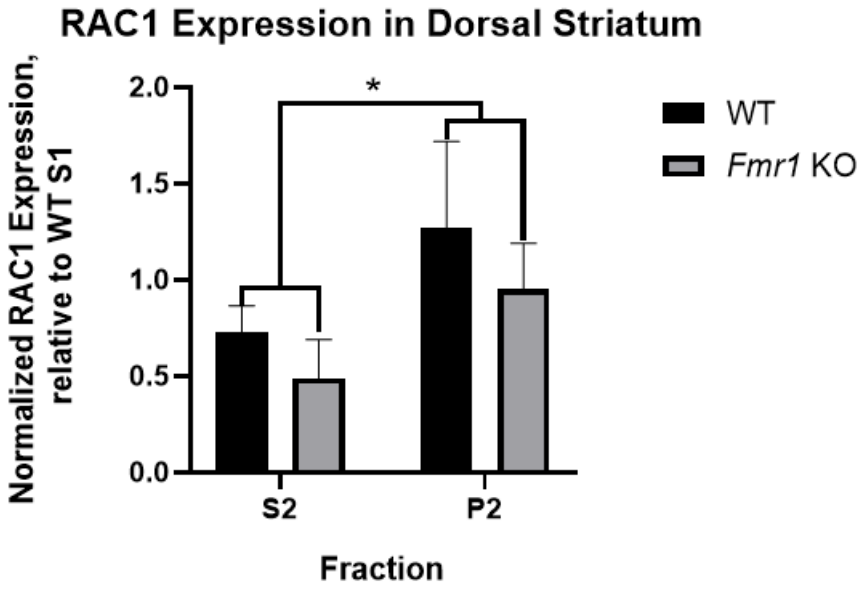

Figure 17: Expression of RAC1 in dorsal striatum in the S2 compared to P2 fraction. KO: n=4; WT: n=4. Two-Way Mixed ANOVA. *p<0.05. Data shown are mean ± SEM.

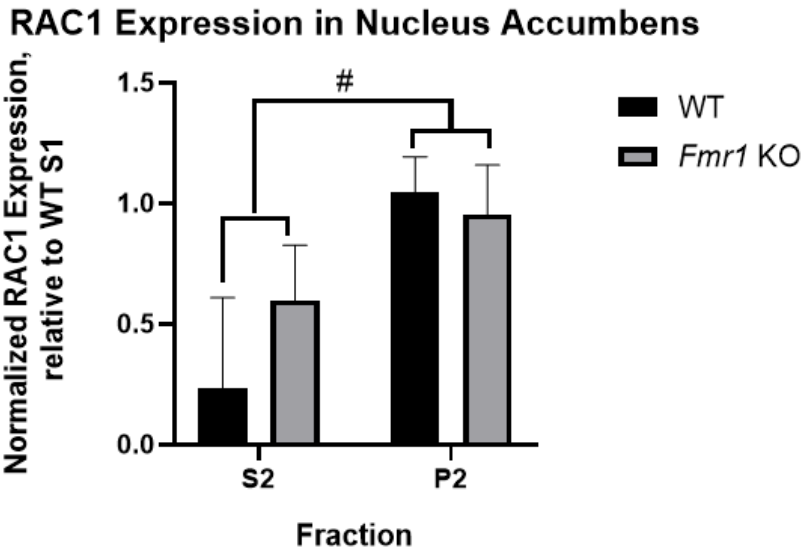

Figure 18: Expression of RAC1 in nucleus accumbens in the S2 and P2 fractions. KO: n=4; WT: n=4. Two-Way Mixed ANOVA. #=0.057. Data shown are mean ± SEM.

3.1.2.3. Behavioral Correlations

Behaviors throughout the food operant conditioning experiment were analyzed to determine if there was any correlation between behavioral responses and protein expression. This analysis was performed for every protein tested using western blots for the S2 and P2 fractions in WT compared to *Fmr1* KO animals. The behaviors analyzed were number of reinforcers earned on day one of acquisition, number of reinforcers earned during each of the last four days of acquisition, number of active port nose pokes on the first day of extinction, number of active port nose pokes on the last day of extinction, number of reinforcers earned on the first day of reacquisition, number of reinforcers earned on the last day of reacquisition, and the average number of reinforcers earned at each dose during dose response testing.

3.1.2.3.1. Acquisition Behaviors

3.1.2.3.1.1. Dorsal Striatum

In dorsal striatum, there was a significant correlation between ARC expression in the S2 fraction and number of reinforcers earned on the last day of acquisition for wild type animals (Pearson's correlation, $r = -0.9588$, $p<0.05$, $n=4$). There were no significant correlations observed in the KO animals when analyzing ARC expression in the S2 fraction. There were also no significant correlations observed when analyzing behavioral correlations and ARC expression in the P2 fraction for WT or KO animals. No significant differences were observed when analyzing the expression of the unspecified ARC band in either the WT or KO animal in either the S2 or P2 fractions.

For RAC1, there was a significant correlation between expression in the P2 fraction of WT animals and number of reinforcers earned in the day prior to the last day of acquisition (Pearson's correlation, $r = 0.9622$, $p<0.05$, $n=4$), as well as with the last day of acquisition (Pearson's correlation, $r = 0.9588$, $p<0.05$, $n=4$). In KO animals, there was a significant correlation between RAC1 in the P2 fraction and the number of reinforcers earned on the fourth to last day of acquisition (Pearson's correlation, $r = -0.9545$, $p<0.05$, $n=4$).

For PSD-95, there was a significant correlation of expression in the P2 fraction of KO animals and the number of reinforcers they earned during the second to last day of extinction (Pearson's correlation, $r = -0.9992$, $p<0.001$, $n=4$), as well as during the last day of extinction (Pearson's correlation, $r = -0.9901$, $p<0.01$, $n=4$). There were no significant correlations in the S2 or P2 fractions of the WT animals. There also were no significant correlations or trends in the S2 fraction of the KO animals.

3.1.2.3.1.2. Nucleus Accumbens

There were no significant correlations when analyzing the expression of ARC in either the S2 or P2 fractions of WT or KO animals. There was a significant correlation between RAC1 expression in the WT S2 fraction and the number of reinforcers earned during the third to last day (Pearson's correlation, $r = 0.9762$, $p<0.05$, $n=4$), the second to last day (Pearson's correlation, $r=0.9867$, $p<0.05$, $n=4$) and the last day (Pearson's correlation, $r = 0.9930$, $p<0.01$, $n=4$). In the P2 fraction of KO animals there was a significant correlation between PSD-95 expression and the number of reinforcers earned during the

second to last day of acquisition (Pearson's correlation, $r = -0.9891$, $p<0.05$, $n=4$) and during the last day of acquisition (Pearson's correlation, $r = -0.9694$, $p<0.05$, $n=4$). There were no significant correlations in the WT animals for PSD-95.

3.1.2.3.2. Extinction

3.1.2.3.2.1. Dorsal Striatum

For ARC, the higher molecular weight band that appeared with Arc, RAC1, and PSD-95 expression in the S2 or P2 fractions, there were no significant correlations with the first day of extinction for either the WT or KO animals.

3.1.2.3.2.2. Nucleus Accumbens

There was a significant correlation between RAC1 expression in the P2 fraction of WT animals and the number of active nose pokes during the first day of extinction (Pearson's correlation, $r = 0.9619$, $p<0.05$, $n=4$). For this region, there were no other significant correlations or trends in any of the tested proteins in either the WT or KO animals in either fraction with extinction-related measures.

3.1.2.3.3. Reacquisition

3.1.2.3.3.1. Dorsal Striatum

There was a significant correlation between ARC expression and the number of reinforcers earned during the first day of reacquisition in the S2 fraction of WT animals (Pearson's correlation, $r = -0.9724$, $p<0.05$, $n=4$).

3.1.2.3.3.2. Nucleus Accumbens

In the P2 fraction of the WT animals, there was a significant correlation between RAC1 expression and the number of reinforcers earned during the first day of reacquisition (Pearson's correlation, $r = 0.9901$, $p<0.01$, $n=4$).

3.1.2.3.4. Dose Response Testing

3.1.2.3.4.1. Dorsal Striatum

In the S2 fraction of WT animals there was a trend towards significant correlation of ARC expression and the average number of reinforcers earned at the three (Pearson's correlation, $r = -0.9002$, $p=0.0998$, $n=4$) and 32 percent (Pearson's correlation, $r = -0.9446$, $p=0.0554$, $n=4$) reinforcer concentrations. In the P2 fraction of the KO animals, there was a significant correlation between ARC expression and the average number of reinforcers earned at the 100 percent concentration (Pearson's correlation, $r = 0.9907$, $p<0.01$, $n=4$). In the S2 fraction of the WT animals, there was a significant correlation between the expression of the unspecified ARC and the average number of reinforcers earned at the 32 percent dose (Pearson's correlation, $r = 0.9528$, $p<0.05$, $n=4$). In the P2 fraction of the KO animals there was a significant correlation between the average number of reinforcers earned at the 100 percent dose and the expression of the unspecified ARC (Pearson's correlation, $r = 0.9907$, $p<0.01$, $n=4$). In the S2 fraction of the KO animals there was a significant correlation between the average number of reinforcers earned and PSD-95 expression (Pearson's correlation, $r=0.9789$, $p<0.05$, $n=4$).

3.1.2.3.4.2. Nucleus Accumbens

In the P2 fraction of the WT animals there was a significant correlation between expression of the unspecified ARC and the average number of reinforcers earned at the 32 percent concentration (Pearson's correlation, $r = 0.9872$, $p<0.05$, $n=4$). In the S2 fraction of the WT animals there was a significant correlation between RAC1 expression and the average number of reinforcers earned at the 32 percent dose (Pearson's correlation, $r = 0.9378$, $p=0.0622$, $n=4$). In the P2 fraction of the WT animals there was a significant correlation between RAC1 expression and the average number of reinforcers earned at the 0 percent dose (Pearson's correlation, $r = 0.9575$, $p<0.05$, $n=4$) and the three percent dose (Pearson's correlation, $r = 0.9583$, $p<0.05$, $n=4$). In the P2 fraction of the KO animals there was a significant correlation between the average number of reinforcers earned at the 100 percent dose and the expression of RAC1 (Pearson's correlation, $r = -0.9783$, $p<0.05$, $n=4$). In the S2 fraction of the KO animals there was a significant correlation between PSD-95 expression and the average number of reinforcers earned at the 0 percent dose (Pearson's correlation, $r=0.9749$, $p<0.05$, $n=4$).

3.2. ChAT-Cre x Fl-*Fmr1* Conditional KO Mice

3.2.1. Immunohistochemistry

3.2.1.1. Co-localization of FMRP and ChAT

Since disruption of the cholinergic system results in behaviors associated with ASD, we first confirmed presence of FMRP in cholinergic cells by immunohistochemical co-staining of ChAT and FMRP in brain slices containing striatum (Figure 19).

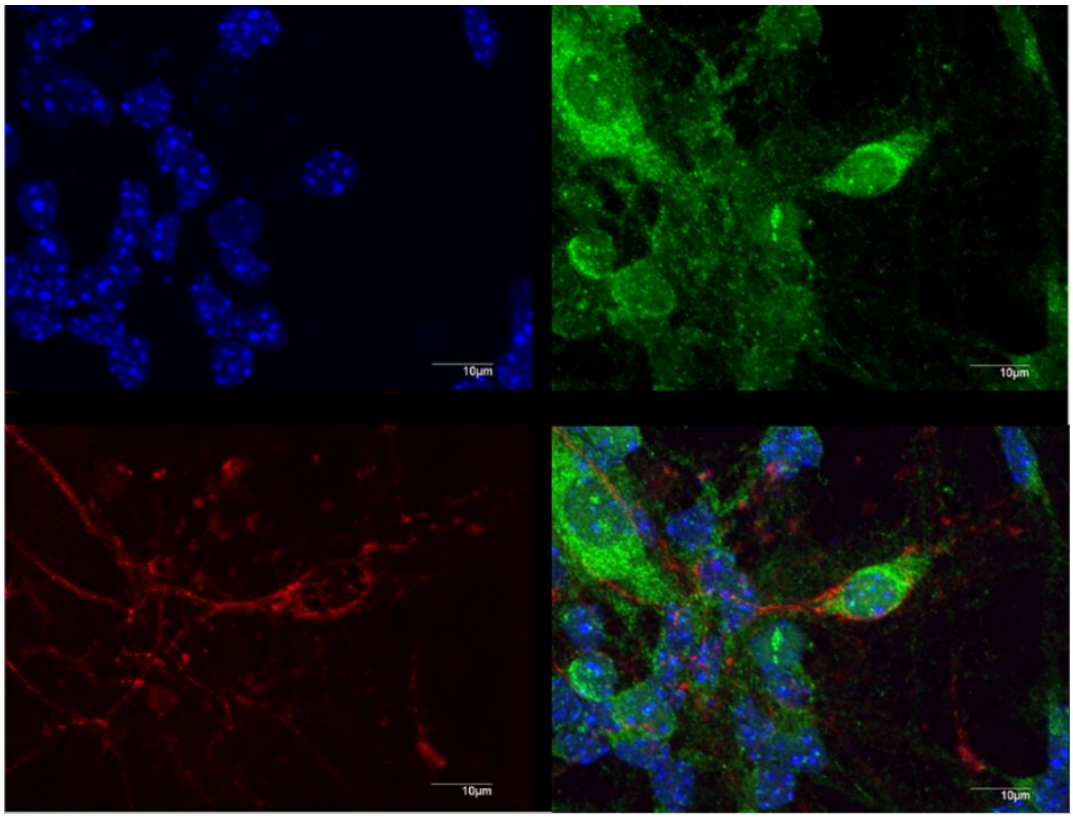

Figure 19: Co-localization of ChAT (red) and FMRP (green). DAPI (nuclei) in blue. Scale bars = 10 µm.

3.2.2. Behavioral Testing

3.2.2.1. Social Conditioned Place Preference.

Comparing the pre- and post-test scores of littermate mice with FMRP either present or conditionally knocked out in the cholinergic cell population, we observed a strong trend towards a significant genotype x test session interaction (Figure 20; Repeated Measures ANOVA, $F_{1,27} = 3.617$, $p=0.068$), where WT mice showed an increase in time spent in the social-paired chamber at the post-test and cKO mice showed a decrease. No significance was observed in follow-up analyses. As with the *Fmr1* KO line, there was a

significant difference in the social-paired chamber entries, due to an increase in chamber entries which held for both genotypes individually (Figure 21; Two-Way Mixed ANOVA $F_{1,27} = 29.28$, $p<0.0001$). There was also a significant increase in entries into the unpaired (non-social) chamber (Figure 22; Two-Way Mixed ANOVA, main effect of test, $F_{1,27} = 21.99$, $p<0.0001$), which again, remained true for each genotype (Bonferroni post-hoc tests, WT $p<0.05$; KO $p<0.01$).

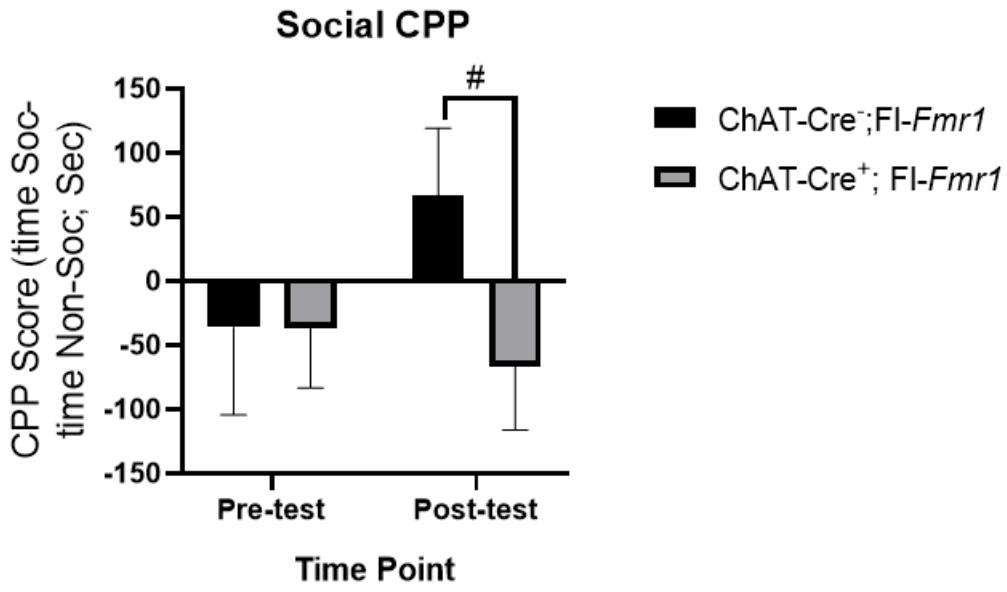

Figure 20: ChAT-Cre^{+};Fl-*Fmr1* and ChAT-Cre^{-};Fl-*Fmr1* scores in both pre- and post-tests. KO: n=16; WT: n=13. RM ANOVA. #=0.0679. Data shown are mean ± SEM.

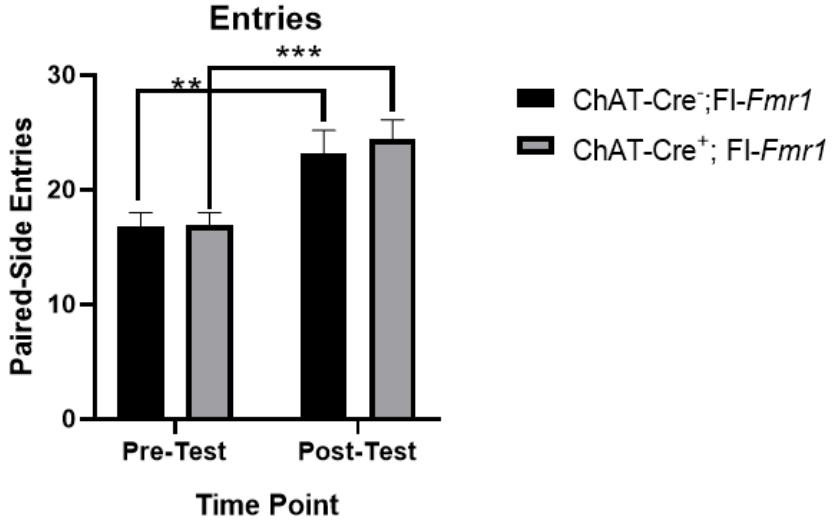

Figure 21: ChAT-Cre^{+};Fl-*Fmr1* and ChAT-Cre^{-}; Fl-*Fmr1* scores in both pre- and post-tests. Two-Way Mixed ANOVA. **p<0.01, ***p<0.001. Data shown are mean ± SEM.

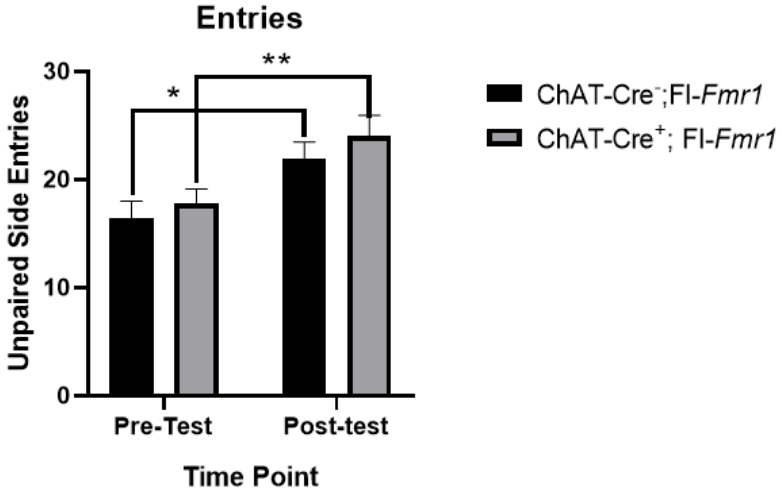

Figure 22: ChAT-Cre^{+};Fl-*Fmr1* and ChAT-Cre^{-};Fl-*Fmr1* mice entries into the unpaired chamber in both pre-and post-tests. KO: n=16; WT: n=13. Two-Way Mixed ANOVA. *p<0.05, **p<0.01. Data shown are mean ± SEM.

3.2.3. Tissue Analysis

3.2.3.1. Social conditioned place preference

Dorsal striatal and nucleus accumbens tissue was collected and synaptosomal and cytoplasmic fractions were prepared from the ChAT; Fl-*Fmr1* cohort, as previously, for western blotting. In the dorsal striatum for ARC, there was a trend towards a main effect of fraction indicating an increase for ARC expression in the P2 fraction (Figure 23; Two-Way Mixed ANOVA, $F_{1,4}$ =5.623, p=0.077). In addition to the ARC band that appeared at the appropriate size, there was the same additional band as was seen in the *Fmr1* KO studies. This band was also analyzed in the *ChAT*-Cre *cohort,* and showed a main effect of fraction due to decreased expression in P2 fraction for the dorsal striatum (Figure 24; Two-Way Mixed ANOVA, $F_{1,4}$ =13.102, p<0.05). For RAC1, there were no significant differences observed (Figure 25). The final protein, PSD-95, showed a trend towards a main effect due to an increase of expression in the P2 fraction compared to that of the S2 fraction (Figure 26; Two-Way Mixed ANOVA, $F_{1,4}$ =7.630, p=0.051).

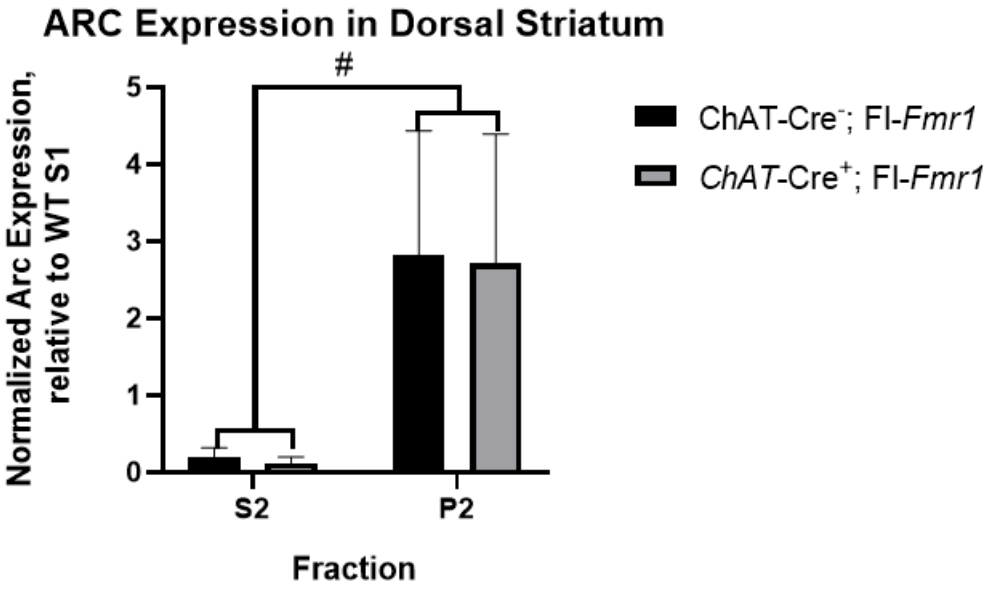

Figure 23: Expression of ARC in the P2 fraction from the ChAT Cre;Fl-Fmr1 study. WT: n=3; KO: n=3. Two-Way Mixed ANOVA. #=0.077. Data shown are mean ± SEM.

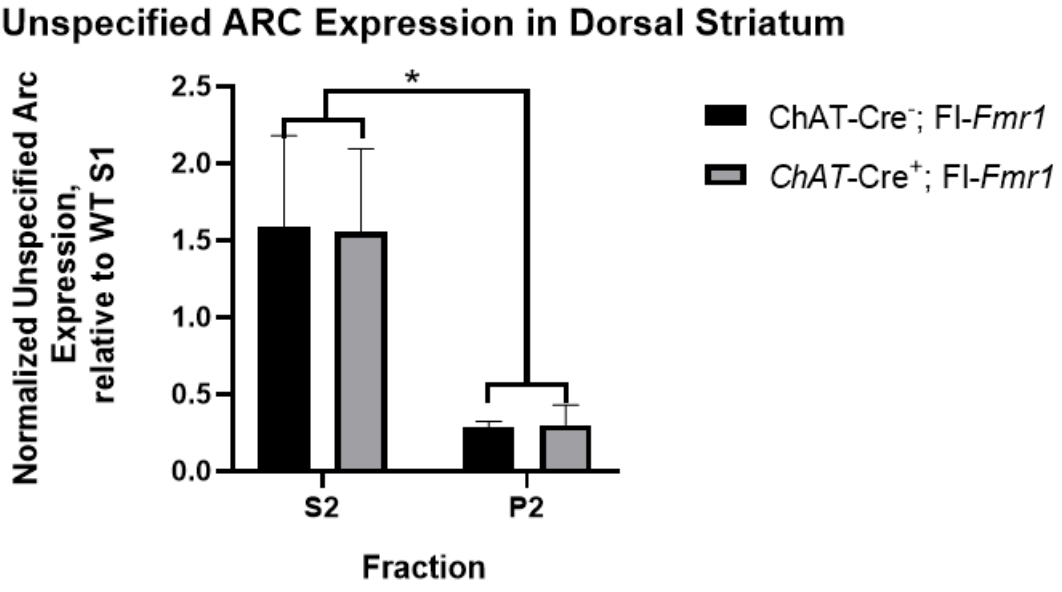

Figure 24: Unspecified ARC expression in the dorsal striatum. KO: n=3; WT: n=3. Two-Way Mixed ANOVA. *p<0.05. Data shown are mean ± SEM.

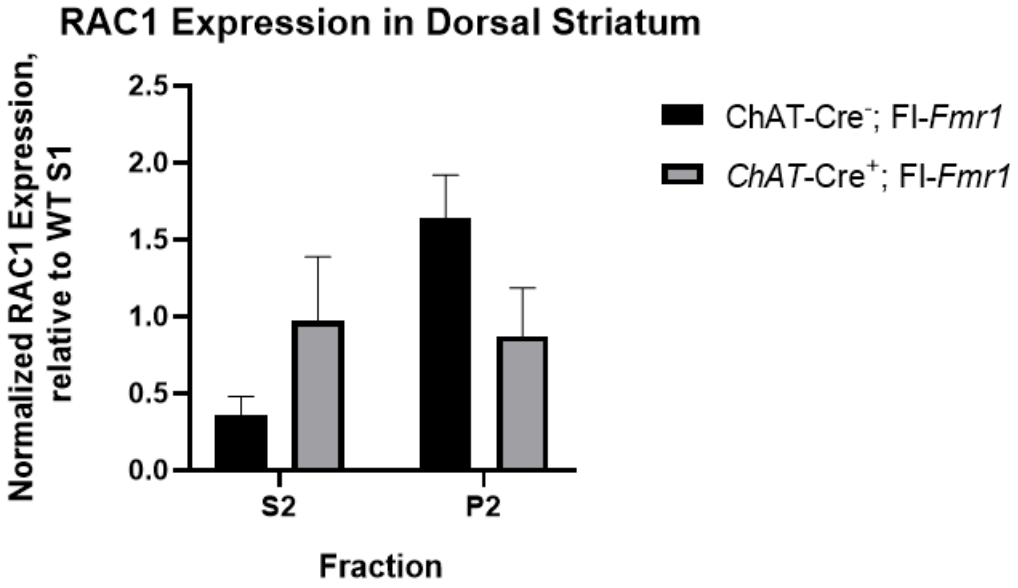

Figure 25: Expression of RAC1 in dorsal striatum. Two-Way Mixed ANOVA. KO: n=3; WT: n=3. Data shown are mean ± SEM.

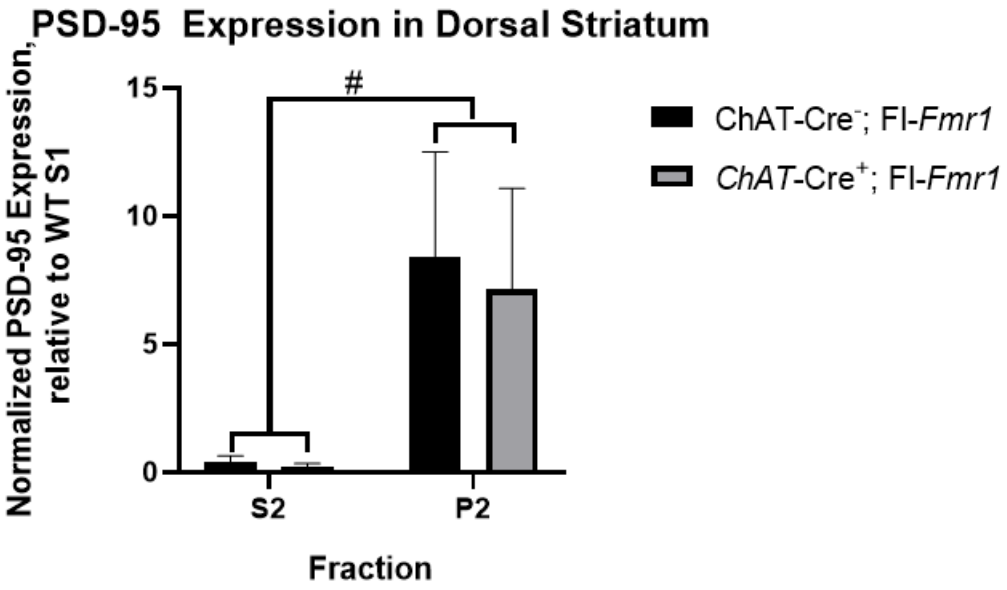

Figure 26: Expression of PSD-95 in the dorsal striatum. KO: n=3; WT: n=3. Two-Way Mixed ANOVA. #=0.051. Data shown are mean ± SEM.

These same proteins were also probed for using tissue from the nucleus accumbens. When analyzing ARC, there was a main effect due to the significant increase of expression in the P2 fraction (Figure 27; Two-Way Mixed ANOVA, $F_{1,4}$ =51.871, $p<0.01$). For the ~130 kDa unidentified band that was present for ARC, there was a main effect of fraction due to the significant decrease of expression in the P2 fraction (Figure 28; Two-Way Mixed ANOVA, $F_{1,4}$ =23.339, $p<0.01$). RAC1 showed no significant difference between genotypes across the S1 fraction. There was a main effect of fraction due to an increased expression within the P2 fraction (Figure 29; Two-Way Mixed ANOVA, $F_{1,4}$=8.704, $p<0.05$). Lastly, PSD-95 showed a trend towards a significant main effect of fraction due to an increased expression in the P2 fraction compared to the S2 fraction (Figure 30; Two-Way Mixed ANOVA, $F_{1,4}$=7.288, $p=0.054$).

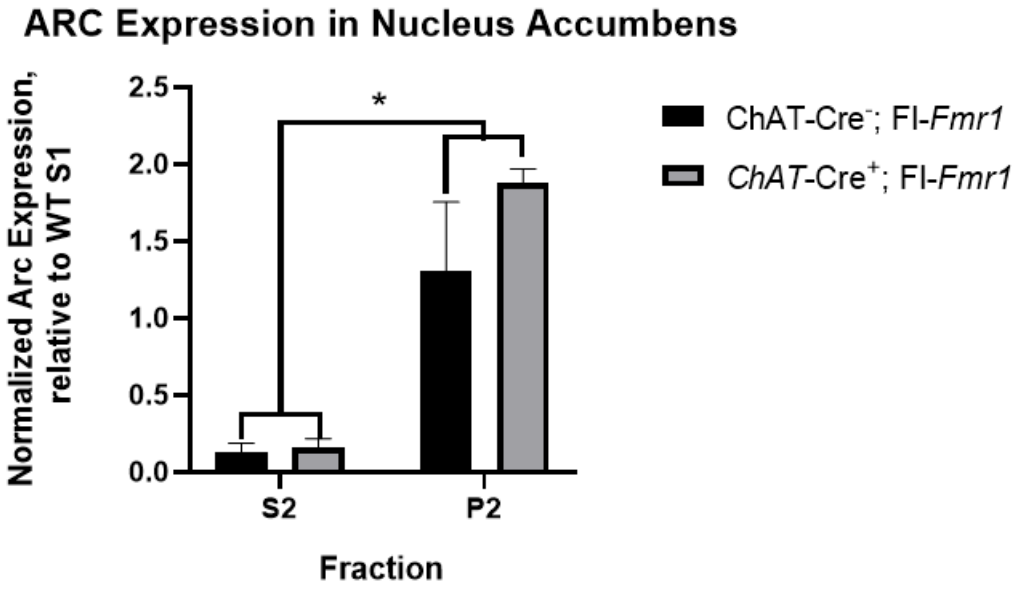

Figure 27**:** ARC expression in the nucleus accumbens in the ChAT-Cre; Fl-***Fmr1*** sCPP study. KO: n=3; WT: n=3. Two-Way Mixed ANOVA. *p<0.05. Data shown are mean ± SEM.

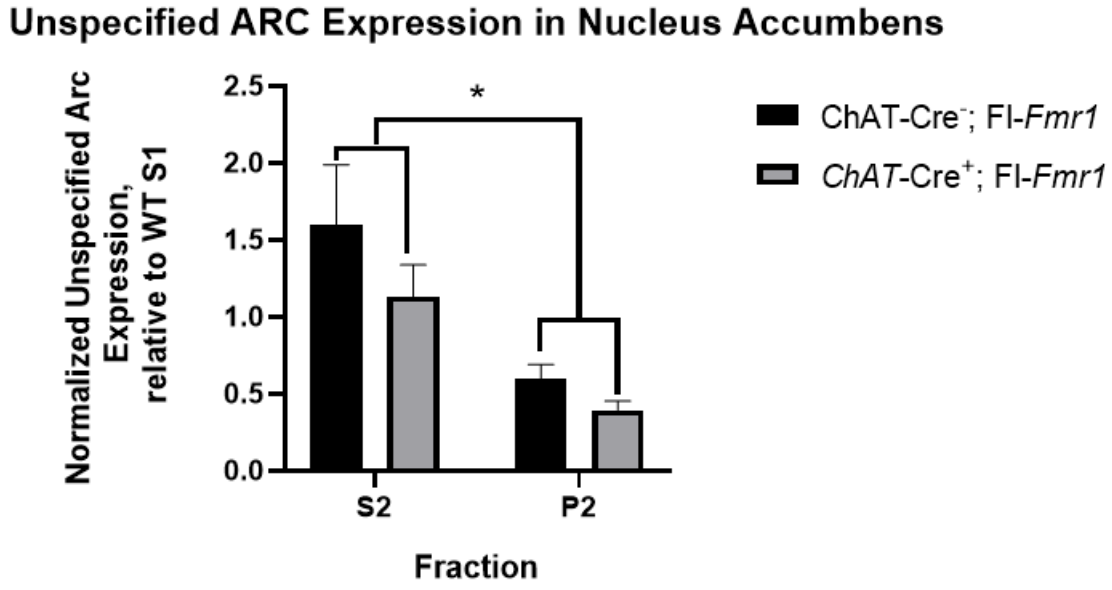

Figure 28: Unspecified ARC expression in the NAc. KO: n=3; WT: n=3. Two-Way Mixed ANOVA. *p<0.01. Data shown are mean ± SEM.

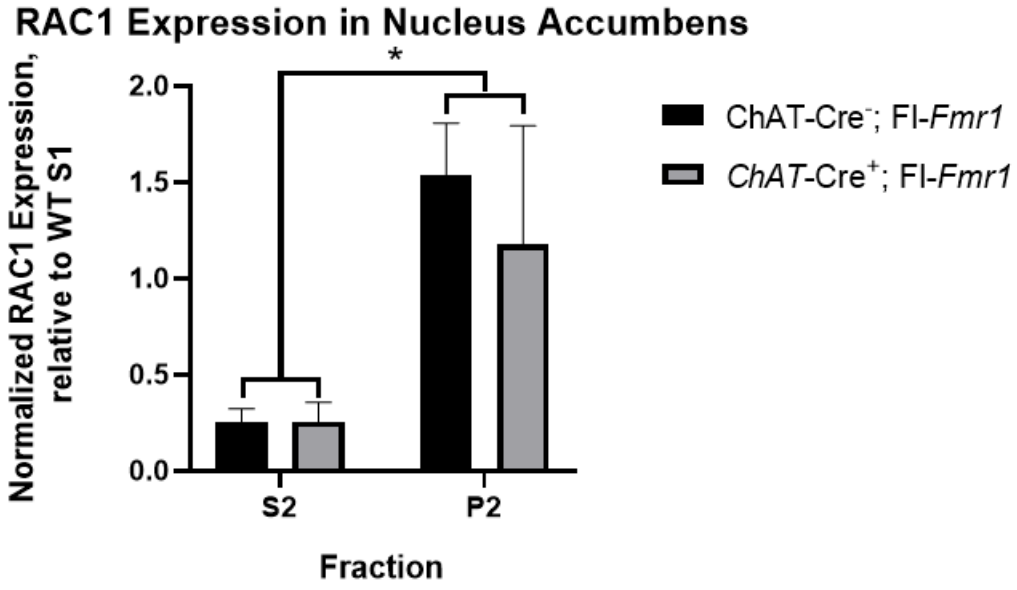

Figure 29: RAC1 expression in the NAc. KO: n=3; WT: n=3. Two-Way Mixed ANOVA. *p<0.05. Data shown are mean ± SEM.

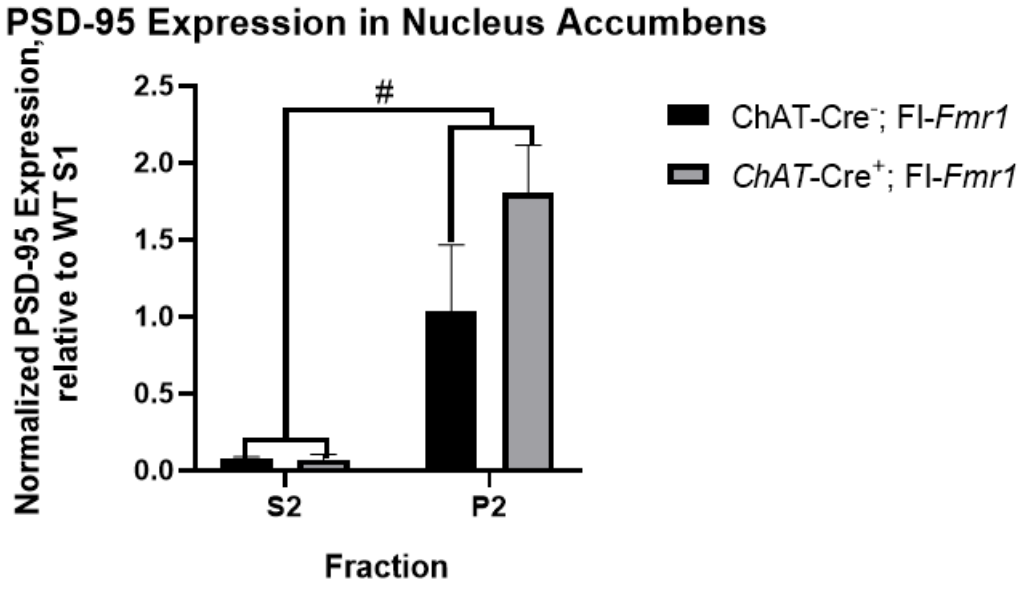

Figure 30: PSD-95 expression in the NAc in the cytosolic and synaptic fractions. KO: n=3; WT: n=3. Two-Way Mixed ANOVA. #=0.054. Data shown are mean ± SEM.

4. DISCUSSION AND CONCLUSIONS

Fragile X syndrome and ASD are associated with social interaction deficits (Cordeiro et al., 2011). To better elucidate reward deficits associated with fragile X syndrome, tests of food and social reward behavior were designed and implemented. Social reward deficits in our test did not reach significance between *Fmr1* WT and KO mice. However, conditional knockout mice lacking FMRP in cholinergic cells showed a strong trend towards a significant deficit in social reward. When using the *Fmr1* KO mouse model in an operant conditioning test involving food reward, only very minor differences were apparent between the two genotypes, suggesting normal natural reward function with regard to palatable food in the mouse model for FXS and basically normal learning and extinction abilities. Using dorsal striatum and nucleus accumbens tissue collected from these mice, further experimentation was performed to identify any potential differences in the striatal expression of FMRP targets between the genotypes.

The social conditioned place preference experiment did not result in a significant difference between *Fmr1* KO and WT mice concerning their preference for the social context, an outcome that we hope to better understand. It is of note that *Fmr1* KO mice did, on average, show mild avoidance of the social-paired chamber during the post-test, while WT mice instead showed a mild preference for this context. We note that in this assay, testing for social preference occurs in the absence of the social companion. Patients diagnosed with FXS have shown decreased social gaze, and are postulated to

suffer more from severe social anxiety than from a genuine lack of reward from social experiences (Hong et al., 2019). In light of this information, it may be that our social CPP paradigm is not optimal for measuring social deficits in fragile X mice.

We also did not see significant reward deficits in *Fmr1* KO mice using a palatable (sweetened, vanilla-flavored liquid) food in the operant conditioning assay. A previous study has shown that loss of FMRP results in impairment of cocaine-induced reward in the CPP assay, but also showed normal learning of CPP induced with a palatable (high-fat solid) food (Smith et al., 2014). The slightly increased responses maintained during extinction by *Fmr1* KO mice in our current assay, along with the slightly longer time frame for the animals to reach threshold for each phase, suggests that there may be a slight learning impairment—not enough to prohibit learning, but enough to delay it.

Interestingly, social deficits were apparent when FMRP was removed specifically from cholinergic cells. Specifically, *ChAT Cre*$^{+}$ *and ChAT Cre*$^{-}$ floxed-*Fmr1* cKO mice showed divergent post-, compared to pre-, test responses for the social-paired chamber, where *ChAT Cre*$^{+}$ floxed-*Fmr1* mice avoided the social-paired chamber. It has previously been shown that loss of acetylcholine increases social deficits, and these deficits can be rescued by increasing acetylcholine levels (Karvat & Kimchi, 2014). Fragile X mice have been noted to have decreased acetylcholine in brain (Davidovic et al., 2011), including specifically in the striatum (Qiu, Chen, Guo, Wu, & Yi, 2016), although we note that the latter study was performed on the FVB mouse background

strain and not the C57BL/6 background that we use. Future studies will needed to study the effects of the loss of FMRP solely in striatal ChAT cells, as well as to further elucidate the effect this loss would have on acetylcholine levels. In addition to the effect on acetylcholine, further analysis of the expression and localization of FMRP's targets in ChAT-expressing striatal cells either having or lacking FMRP is warranted.

When we examined protein expression of FMRP targets in the *Fmr1* KO and WT mice that underwent food operant conditioning, ARC was significantly increased in the P2 fraction, showing higher synaptic localization. ARC has been shown to be increased at the basal level in KO hippocampal neurons (Niere et al., 2012), a finding we did not observe in our striatal samples. The non-specific ARC band was significantly higher in the S2 fraction in both KO and WT animals in the dorsal striatum, and in the nucleus accumbens, was significantly increased in KO, while trending towards significance in WT, animals, showing an increased localization to the cytosol in striatum. While it is not yet clear the significance of this band, dimers and trimers of ARC have been observed using crosslinking assays, suggesting they may occur under normal cellular conditions. To determine whether the higher molecular weight ARC band we are observing has functional relevance, future work will need to use these or similar techniques to explore this question in the context of our mouse model. PSD-95 was either trending toward a significant increase in the P2 fraction, as seen in the dorsal striatum of both genotypes for the total *Fmr1* KO mouse line, as well as in the dorsal striatum and NAc of the ChAT; Fl-*Fmr1* mice, or was significantly increased, as seen in the NAc P2 fractions of

the *Fmr1* KO line. FMRP has been implicated in the stabilization of PSD-95 mRNA using samples of whole brain (Zalfa et al., 2007), and though there is not a significant difference, on average, the KO animals showed lower expression of PSD-95. RAC1 levels of the KO animals compared to the WT animals varied across region, but this difference never reached the level of significance. FMRP is thought to be a negative regulator of RAC1, based on studies in the hippocampus, so an increase of RAC1 may be expected (Bongmba, Martinez, Elhardt, Butler, & Tejada-Simon, 2011). However, no evidence of this was observed in our protein analyses of striatal regions.

In mice that underwent social CPP, qPCR analysis showed a trend toward significantly increased *Dgkκ* expression in *Fmr1* KO animals. Interestingly, when observing the amplification curves of *Dgkκ* and *Rac1*, there was clear separation between KO and WT animals in each, providing a visual identification of genotype based on gene expression. There were three animals, however, that showed amplification curves more like the other genotype—an effect that interestingly, also applied to their social CPP scores. There was no significant difference in *Arc* expression between the genotypes. In the NAc, we found *Shank2* to be significantly decreased in *Fmr1* KO compared to WT mice with only two mice in each group. Although we will need to add animals to this analysis to be certain of this finding, it is suggestive of FMRP playing a critical role in *Shank2* mRNA stabilization in striatal brain regions. Others have suggested that FMRP may play more of a direct role in transcriptional regulation. For example, this possibility for FMRP has been suggested for specific transcripts such as *Necdin*, or NDN (Liu et al., 2018). The

authors of this study suggested that genes involved in neurogenesis are mainly altered at the mRNA level, while synaptic genes are more often regulated at the translational level with adjustments occurring at each end. Here, our RNA findings could be the result of changes in translation efficiency due to loss of FMRP, or due to loss of FMRP's translational regulation feeding back on transcriptional processes, but they do not rule out a direct role for FMRP in transcriptional regulation.

Here our behavioral assays further elucidate behaviors associated FXS and ASD, resulting in considerations for future research. The more pronounced social aversion in the *ChAT*; Fl-*Fmr1* line, in particular, may provide insight into the cellular pathways prominently involved in FXS, and the protein and RNA studies further illuminate the complexities of FMRP's varied regulatory functions. Future studies should further elucidate FMRP's role in the regulation of select targets, between transcription and translation.

REFERENCES

Abitbol, M., Menini, C., Anne-Lise, D., Rhyner, T., Vekemans, M., & Mallet, J. (1993). Nucleus basalis magnocellularis and hippocampus are the major sites of FMR-1 expression in the fetal brain. *Nature Genetics, 4*, 147-153.

Ashley, C. T. J., Wilkinson, K., Reines, D., & Warren, S. (1993). FMR1 protein: Conserved RNP family domains and selective RNA binding. *Science, 262*, 563-566.

Balleine, B. W., Liljeholm, M., & Ostlund, S. B. (2009). The integrative function of the basal ganglia in instrumental conditioning. *Behavioural Brain Research, 199*(1), 43-52.

Ballinger, E. C., Cordeiro, L., Chavez, A. D., Hagerman, R. J., & Hessl, D. (2014). Emotion potentiated startle in fragile X syndrome. *Journal of Autism and Developmental Disorders, 44*(10), 2536-2546.

Bardoni, B., Sittler, A., Shen, Y., & Mandel, J. L. (1997). Analysis of domains affecting intracellular localization of the FMRP protein. *Neurobiology of Disease, 4*(5), 329-336.

Berry-Kravis, E., & Potanos, K. (2004). Psychopharmacology in fragile X syndrome - present and future. *Mental Retardation and Developmental Disabilities Research Reviews, 10*, 42-48.

Bongmba, O. Y. N., Martinez, L. A., Elhardt, M. E., Butler, K., & Tejada-Simon, M. V. (2011). Modulation of dendritic spines and synaptic function by Rac1: A possible link to fragile X syndrome pathology. *Brain Research, 1399*, 79-95.

Borghgraef, M., Fryns, J. P., Dlelkens, A., Pyck, K., & Berghe, H. V. D. (1987). Fragile (X) syndrome: A study of the psychological profile in 23 prepubertal patients. *Clinical Genetics, 32*(3), 179-186.

Bregman, J. D., Leckman, J. F., & Ort, S. I. (1988). Fragile X syndrome: Genetic predisposition to psychopathology. *Journal of Autism and Developmental Disorders, 18*(3), 343-354.

Briones, B. A., Tang, V. D., Haye, A. E., & Gould, E. (2018). Response learning stimulates dendritic spine growth on dorsal striatal medium spiny neurons. *Neurobiology of Learning and Memory, 155*, 50-59.

Brown, V., Jin, P., Ceman, S., Darnell, J. C., O'Donnell, W. T., Tenenbaum, S. A., . . . Warren, S. T. (2001). Microarray identification of FMRP-associated brain mRNAs and altered mRNA translational profiles in fragile X syndrome. *Cell, 107*(4), 477-487.

Castets, M., Schaeffer, C. l., Bechara, E., Schenck, A., Khandjian, E. W., Luche, S., . . . Bardoni, B. (2005). FMRP interferes with the Rac1 pathway and controls actin cytoskeleton dynamics in murine fibroblasts. *Human Molecular Genetics, 14*(6), 835-844.

Ceman, S., O'Donnell, W. T., Reed, M., Patton, S., Pohl, J., & Warren, S. T. (2003). Phosphorylation influences the translation state of FMRP-associated polyribosomes. *Human Molecular Genetics, 12*(24), 3295-3305.

Chang, S., Bray, S. M., Li, Z., Zarnescu, D. C., He, C., Jin, P., & Warren, S. T. (2008). Identification of small molecules rescuing fragile X syndrome phenotypes in Drosophila. *Nature Chemical Biology, 4*(4), 256-263.

Chen, L., Yun, S. W., Seto, J., Liu, W., & Toth, M. (2003). The fragile X mental retardation protein binds and regulates a novel class of mRNAs containing u rich target sequences. *Neuroscience, 120*(4), 1005-1017.

Chuang, S.-C., Zhao, W., Bauchwitz, R., Yan, Q., Bianchi, R., & Wong, R. K. S. (2005). Prolonged epileptiform discharges induced by altered group I metabotropic glutamate receptor-mediated synaptic responses in hippocampal slices of a fragile X mouse model. *The Journal of Neuroscience, 25*(35), 8048-8055.

Cohen, I. (1995). Behavioral profiles of autistic and nonautistic fragile X males. *Developmental Brain Dysfunction*, 252-269.

Cohen, I., Fisch, G., Sudhalter, V., G Wolf-Schein, E., Hanson, D., Hagerman, R., . . . Brown, W. (1988). Social gaze, social avoidance, and repetitive behavior in fragile X males: A controlled study. *American Journal of Mental Retardation, 92*, 436-446.

Comery, T. A., Harris, J. B., Willems, P. J., Oostra, B. A., Irwin, S. A., Weiler, I. J., & Greenough, W. T. (1997). Abnormal dendritic spines in fragile X knockout mice: Maturation and pruning deficits. *Proceedings of the National Academy of Sciences of the United States of America, 94*(10), 5401-5404.

Corbin, F., Bouillon, M., Fortin, A., Morin, S., Rousseau, F., & Khandjian, E. W. (1997). The fragile X mental retardation protein is associated with poly(A)+ mRNA in actively translating polyribosomes. *Human Molecular Genetics, 6*(9), 1465-1472.

Cordeiro, L., Ballinger, E., Hagerman, R., & Hessl, D. (2011). Clinical assessment of DSM-IV anxiety disorders in fragile X syndrome: Prevalence and characterization. *Journal of Neurodevelopmental Disorders, 3*(1), 57-67.

D'Antuono, M., Merlo, D., & Avoli, M. (2003). Involvement of cholinergic and gabaergic systems in the fragile X knockout mice. *Neuroscience, 119*(1), 9-13.

Darnell, Jennifer C., Van Driesche, Sarah J., Zhang, C., Hung, Ka Ying S., Mele, A., Fraser, Claire E., . . . Darnell, Robert B. (2011). FMRP stalls ribosomal translocation on mRNAs linked to synaptic function and autism. *Cell, 146*(2), 247-261.

Davidovic, L., Navratil, V., Bonaccorso, C. M., Catania, M. V., Bardoni, B., & Dumas, M. E. (2011). A metabolomic and systems biology perspective on the brain of the fragile X syndrome mouse model. *Genome Research, 21*(12), 2190-2202.

de Vries, B. B., Wiegers, A. M., Smits, A. P., Mohkamsing, S., Duivenvoorden, H. J., Fryns, J. P., . . . Niermeijer, M. F. (1996). Mental status of females with an FMR1 gene full mutation. *American Journal of Human Genetics, 58*(5), 1025-1032.

Demark, J. L., Feldman, M. A., & Holden, J. J. A. (2003). Behavioral relationship between autism and fragile X syndrome. *American Journal on Mental Retardation, 108*(5), 314-326.

Dictenberg, J. B., Swanger, S. A., Antar, L. N., Singer, R. H., & Bassell, G. J. (2008). A direct role for FMRP in activity-dependent dendritic mRNA transport links filopodial-spine morphogenesis to fragile X syndrome. *Developmental Cell, 14*(6), 926-939.

Ding, J. B., Guzman, J. N., Peterson, J. D., Goldberg, J. A., & Surmeier, D. J. (2010). Thalamic gating of corticostriatal signaling by cholinergic interneurons. *Neuron, 67*(2), 294-307.

Dölen, G., Osterweil, E., Rao, B. S. S., Smith, G. B., Auerbach, B. D., Chattarji, S., & Bear, M. F. (2007). Correction of fragile X syndrome in mice. *Neuron, 56*(6), 955-962.

Eberhart, D. E., Malter, H. E., Feng, Y., & Warren, S. T. (1996). The fragile X mental retardation protein is a ribonucleoprotein containing both nuclear localization and nuclear export signals. *Human Molecular Genetics, 5*(8), 1083-1091.

Edbauer, D., Neilson, J. R., Foster, K. A., Wang, C.-F., Seeburg, D. P., Batterton, M. N., . . . Sheng, M. (2010). Regulation of synaptic structure and function by FMRP-associated microRNAs miR-125b and miR-132. *Neuron, 65*(3), 373-384.

Fu, Y.-H., Kuhl, D. P. A., Pizzuti, A., Pieretti, M., Sutcliffe, J. S., Richards, S., . . . Caskey, C. T. (1991). Variation of the CGG repeat at the fragile X site results in genetic instability: Resolution of the Sherman paradox. *Cell, 67*(6), 1047-1058.

Garber, K., Smith, K. T., Reines, D., & Warren, S. T. (2006). Transcription, translation and fragile X syndrome. *Current Opinion in Genetics & Development, 16*(3), 270-275.

Goldberg, J., Ding, J., & Surmeier, D. (2012). Muscarinic modulation of striatal function and circuitry. *Handbook of Experimental Pharmacology, 208*, 223-241.

Greicius, M. D., Boyett-Anderson, J. M., Menon, V., & Reiss, A. L. (2004). Reduced basal forebrain and hippocampal activation during memory encoding in girls with fragile X syndrome. *NeuroReport, 15*(10), 1579-1583.

Hagerman, R., Kemper, M., & Hudson, M. (1985). Learning disabilities and attentional problems in boys with the fragile X syndrome. *American Journal of Diseases of Children, 139*(7), 674-678.

Hagerman, R. J., & Hagerman, P. J. (2002). *Fragile X syndrome: Diagnosis, treatment, and research*. Baltimore: Johns Hopkins University Press.

Hagerman, R. J., Van Housen, K., Smith, A. C., & McGavran, L. (1984). Consideration of connective tissue dysfunction in the fragile X syndrome. *American Journal of Medical Genetics, 17*(1), 111-121.

Hong, M. P., Eckert, E. M., Pedapati, E. V., Shaffer, R. C., Dominick, K. C., Wink, L. K., . . . Erickson, C. A. (2019). Differentiating social preference and social anxiety phenotypes in fragile X syndrome using an eye gaze analysis: A pilot study. *Journal of Neurodevelopmental Disorders, 11*(1), 1-10.

Huber, K. M., Gallagher, S. M., Warren, S. T., & Bear, M. F. (2002). Altered synaptic plasticity in a mouse model of fragile X mental retardation. *Proceedings of the National Academy of Sciences, 99*(11), 7746-7750.

Irwin, S. A., Patel, B., Idupulapati, M., Harris, J. B., Crisostomo, R. A., Larsen, B. P., . . . Greenough, W. T. (2001). Abnormal dendritic spine characteristics in the temporal and visual cortices of patients with fragile-X syndrome: A quantitative examination. *American Journal of Medical Genetics, 98*(2), 161-167.

Karvat, G., & Kimchi, T. (2014). Acetylcholine elevation relieves cognitive rigidity and social deficiency in a mouse model of autism. *Neuropsychopharmacology, 39*(4), 831-840.

Kaufmann, W. E., Cortell, R., Kau, A. S. M., Bukelis, I., Tierney, E., Gray, R. M., . . . Stanard, P. (2004). Autism spectrum disorder in fragile X syndrome: Communication, social interaction, and specific behaviors. *American Journal of Medical Genetics, 129A*(3), 225-234.

Kaufmann, W. E., Kidd, S. A., Andrews, H. F., Budimirovic, D. B., Esler, A., Haas-Givler, B., . . . Berry-Kravis, E. (2017). Autism spectrum disorder in fragile X syndrome: Cooccurring conditions and current treatment. *Pediatrics, 139*(Supplement 3), S194-S206.

Kawaguchi, Y. (1997). Neostriatal cell subtypes and their functional roles. *Neuroscience Research, 27*(1), 1-8.

Kawaguchi, Y., Wilson, C. J., Augood, S. J., & Emson, P. C. (1995). Striatal interneurones: Chemical, physiological and morphological characterization. *Trends in Neurosciences, 18*(12), 527-535.

Kolehmainen, K. (1994). Population genetics of fragile X: A multiple allele model with variable risk of CGG repeat expansion. *American Journal of Medical Genetics, 51*(4), 428-435.

Korb, E., Herre, M., Zucker-Scharff, I., Gresack, J., Allis, C. D., & Darnell, R. B. (2017). Excess translation of epigenetic regulators contributes to fragile X syndrome and is alleviated by Brd4 inhibition. *Cell, 170*(6), 1209-1223.e1220.

Krawczun, M. S., Jenkins, E. C., & Brown, W. T. (1985). Analysis of the fragile-X chromosome: Localization and detection of the fragile site in high resolution preparations. *Human Genetics, 69*(3), 209-211.

Laggerbauer, B., Ostareck, D., Keidel, E.-M., Ostareck-Lederer, A., & Fischer, U. (2001). Evidence that fragile X mental retardation protein is a negative regulator of translation. *Human Molecular Genetics, 10*(4), 329-338.

Li, Z., Zhang, Y., Ku, L., Wilkinson, K. D., Warren, S. T., & Feng, Y. (2001). The fragile X mental retardation protein inhibits translation via interacting with mRNA. *Nucleic Acids Research, 29*(11), 2276-2283.

Liu, B., Li, Y., Stackpole, E. E., Novak, A., Gao, Y., Zhao, Y., . . . Richter, J. D. (2018). Regulatory discrimination of mRNAs by FMRP controls mouse adult neural stem cell differentiation. *Proceedings of the National Academy of Sciences, 115*(48), E11397-E11405.

Miyashiro, K. Y., Beckel-Mitchener, A., Purk, T. P., Becker, K. G., Barret, T., Liu, L., . . . Eberwine, J. (2003). RNA cargoes associating with FMRP reveal deficits in cellular functioning in Fmr1 null mice. *Neuron, 37*(3), 417-431.

Narayanan, U., Nalavadi, V., Nakamoto, M., Pallas, D. C., Ceman, S., Bassell, G. J., & Warren, S. T. (2007). FMRP phosphorylation reveals an immediate-early signaling pathway triggered by group I mGluR and mediated by PP2A. *The Journal of Neuroscience, 27*(52), 14349-14357.

Niere, F., Wilkerson, J. R., & Huber, K. M. (2012). Evidence for a fragile X mental retardation protein-mediated translational switch in metabotropic glutamate receptor-triggered Arc translation and long-term depression. *The Journal of Neuroscience, 32*(17), 5924-5936.

Osterweil, E. K., Krueger, D. D., Reinhold, K., & Bear, M. F. (2010). Hypersensitivity to mGluR5 and ERK1/2 leads to excessive protein synthesis in the hippocampus of a mouse model of fragile X syndrome. *Journal of Neuroscience, 30*(46), 15616-15627.

Peebles, C. L., Yoo, J., Thwin, M. T., Palop, J. J., Noebels, J. L., & Finkbeiner, S. (2010). Arc regulates spine morphology and maintains network stability in vivo. *Proceedings of the National Academy of Sciences, 107*(42), 18173-18178.

Pfeiffer, B. E., Zang, T., Wilkerson, J. R., Taniguchi, M., Maksimova, M. A., Smith, L. N., . . . Huber, K. M. (2010). Fragile X mental retardation protein is required for synapse elimination by the activity-dependent transcription factor MEF2. *Neuron, 66*(2), 191-197.

Pieretti, M., Zhang, F., Fu, Y.-H., Warren, S. T., Oostra, B. A., Caskey, C. T., & Nelson, D. L. (1991). Absence of expression of the FMR-1 gene in fragile X syndrome. *Cell, 66*(4), 817-822.

Qin, M., Kang, J., Burlin, T. V., Jiang, C., & Smith, C. B. (2005). Postadolescent changes in regional cerebral protein synthesis: An in vivo study in the FMR1 null mouse. *Journal of Neuroscience, 25*(20), 5087-5095.

Qiu, G., Chen, S., Guo, J., Wu, J., & Yi, Y. H. (2016). Alpha-asarone improves striatal cholinergic function and locomotor hyperactivity in Fmr1 knockout mice. *Behavioral Brain Research, 312*, 212-218.

Rapanelli, M., Frick, L. R., Xu, M., Groman, S. M., Jindachomthong, K., Tamamaki, N., . . . Pittenger, C. (2017). Targeted interneuron depletion in the dorsal striatum produces autism-like behavioral abnormalities in male but not female mice. *Biological Psychiatry, 82*(3), 194-203.

Ravi, Vijayalaxmi, Gross, C., Yao, X., Xing, L., Laur, O., . . . Gary. (2011). Reversible inhibition of PSD-95 mRNA translation by miR-125a, FMRP phosphorylation, and mGluR signaling. *Molecular Cell, 42*(5), 673-688.

Rudelli, R. D., Brown, W. T., Wisniewski, K., Jenkins, E. C., Laure-Kamionowska, M., Connell, F., & Wisniewski, H. M. (1985). Adult fragile X syndrome. Clinico-neuropathologic findings. *Acta Neuropathologica, 67*(3-4), 289-295.

Sarter, M., Bruno, J. P., & Givens, B. (2003). Attentional functions of cortical cholinergic inputs: What does it mean for learning and memory? *Neurobiology of Learning and Memory, 80*(3), 245-256.

Siomi, H., Siomi, M. C., Nussbaum, R. L., & Dreyfuss, G. (1993). The protein product of the fragile X gene, FMR1, has characteristics of an RNA-binding protein. *Cell, 74*(2), 291-298.

Smith, L. N., Jedynak, J. P., Fontenot, M. R., Hale, C. F., Dietz, K. C., Taniguchi, M., . . . Cowan, C. W. (2014). Fragile X mental retardation protein regulates synaptic and behavioral plasticity to repeated cocaine administration. *Neuron, 82*(3), 645-658.

Tabet, R., Moutin, E., Becker, J. A., Heintz, D., Fouillen, L., Flatter, E., . . . Moine, H. (2016). Fragile X mental retardation protein (FMRP) controls diacylglycerol kinase activity in neurons. *Proceedings of the National Academy of Sciences of the United States of America, 113*(26), E3619-3628.

Tashiro, A., & Yuste, R. (2004). Regulation of dendritic spine motility and stability by Rac1 and Rho kinase: Evidence for two forms of spine motility. *Molecular and Cellular Neuroscience, 26*(3), 429-440.

Tepper, J. M., Tecuapetla, F., Koós, T., & Ibáñez-Sandoval, O. (2010). Heterogeneity and diversity of striatal GABAergic interneurons. *Frontiers in Neuroanatomy, 4*, 150-150.

Todd, P. K., Mack, K. J., & Malter, J. S. (2003). The fragile X mental retardation protein is required for type-I metabotropic glutamate receptor-dependent translation of PSD-95. *Proceedings of the National Academy of Sciences of the United States of America, 100*(24), 14374-14378.

Turner, G., Webb, T., Wake, S., & Robinson, H. (1996). Prevalence of fragile X syndrome. *American Journal of Medical Genetics, 64*(1), 196-197.

Wang, Z., Kai, L., Day, M., Ronesi, J., Yin, H. H., Ding, J., . . . Surmeier, D. J. (2006). Dopaminergic control of corticostriatal long-term synaptic depression in medium spiny neurons is mediated by cholinergic interneurons. *Neuron, 50*(3), 443-452.

Westmark, C. J., & Malter, J. S. (2007). FMRP mediates mGluR5-dependent Translation of amyloid precursor protein. *Pubic Library of Science Biology, 5*(3), e52.

Winter, R. M. (1987). Population genetics implications of the premutation hypothesis for the generation of the fragile X mental retardation gene. *Human Genetics, 75*(3), 269-271.

Zalfa, F., Eleuteri, B., Dickson, K. S., Mercaldo, V., De Rubeis, S., di Penta, A., . . . Bagni, C. (2007). A new function for the fragile X mental retardation protein in regulation of PSD-95 mRNA stability. *Nature Neuroscience, 10*(5), 578-587.

Zalfa, F., Giorgi, M., Primerano, B., Moro, A., Di Penta, A., Reis, S., . . . Bagni, C. (2003). The fragile X syndrome protein FMRP associates with BC1 RNA and regulates the translation of specific mRNAs at synapses. *Cell, 112*(3), 317-327.

Zaslavsky, K., Zhang, W.-B., McCready, F. P., Rodrigues, D. C., Deneault, E., Loo, C., . . . Ellis, J. (2019). SHANK2 mutations associated with autism spectrum disorder cause hyperconnectivity of human neurons. *Nature Neuroscience, 22*(4), 556-564.

Zhou, F. M., Wilson, C. J., & Dani, J. A. (2002). Cholinergic interneuron characteristics and nicotinic properties in the striatum. *Journal of Neurobiology, 53*(4), 590-605.

APPENDIX A

SUPPLEMENTAL FIGURES

Figure A.1: Social conditioned place preference box. The conditioning chambers are those identified by the all grey walls or the stiped siding. The neutral chamber is located at the bottom of the image with the all-white siding.

Figure A.2: Food operant conditioning chamber.

Figure A.3: Inactive and active nose ports located within the operant chamber separated by the reward magazine.

Primer	Direction	Sequence 5'-3'
ARC Variant 1	Forward	CAGTGATTCATACCAGTGAAGAAG
ARC Variant 1	Reverse	GTGATGCCCTTTCCAGACAT
ARC Variant 2	Forward	GAGCCAGGAGAATGACACCA
ARC Variant 2	Reverse	GTGATGCCCTTTCCAGACAT
DGKK	Forward	CCGTTTTCGTGTTCTGGTTT
DGKK	Reverse	CACGAGCGAGATCATTACCA
GAPDH	Forward	AGGTCGGTGTGAACGGATTTG
GAPDH	Reverse	TGTAGACCATGTAGTTGAGGTCA
RAC1	Forward	CCATCAAGTGTGTGGTGGTG
RAC1	Reverse	AACTGATGAGCAGGCAGGTT
SHANK2	Forward	GCAGATGAACAGGGGGAAAT
SHANK2	Reverse	GCTCAATTCCGTTGGTGAAA

Figure A.4: List of primers and their corresponding sequences along with the directionality of the primer.

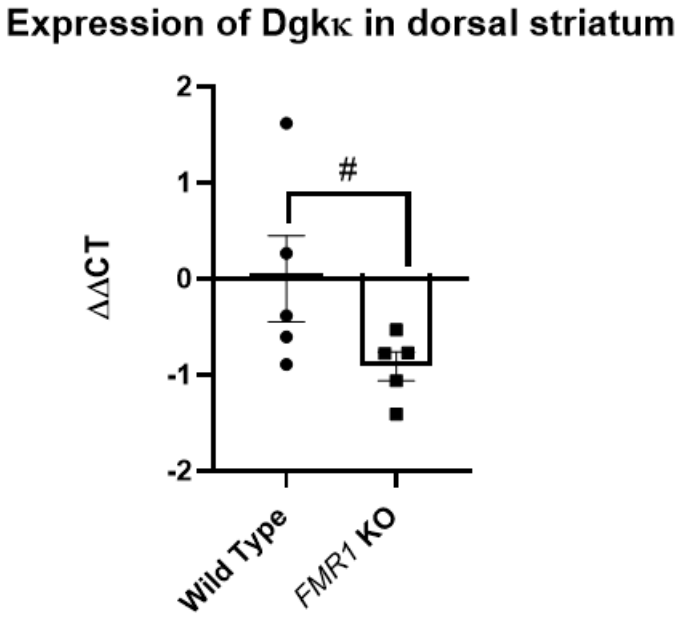

Figure A.5: Expression of Dgkκ in the dorsal striatum. Ct values normalized to GAPDH. WT: n=5; KO: n=5. Mann Whitney U Test. #p=0.0952.

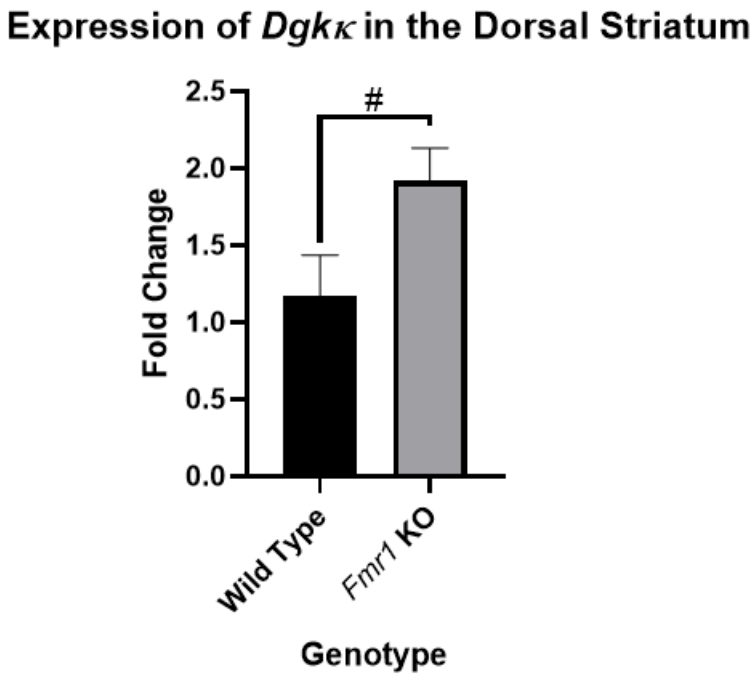

Figure A.6: Expression of Dgkκ in the dorsal striatum. Ct values normalized to GAPDH. WT: n=5; KO: n=5. Mann Whitney U Test. #p=0.0952.

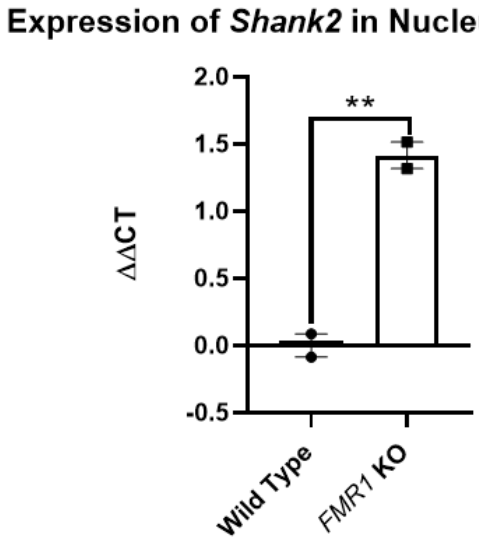

Figure A. 7: Expression of Shank2 in the nucleus accumbens. Ct values normalized to GAPDH. Unpaired t-test. *p<0.01. WT: n=2; KO: n=2.

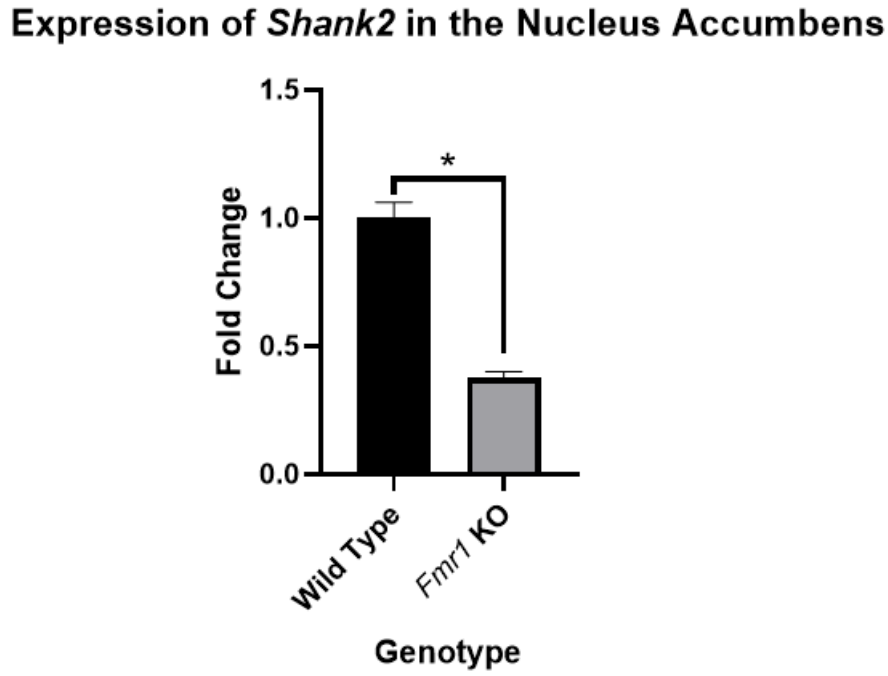

Figure A.8: Expression of Shank2 in the nucleus accumbens. Ct values normalized to GAPDH. Unpaired t-test. *p<0.01. WT: n=2; KO: n=2.